10

Molecular machines

FRANÇISCO M. RAYMO AND J. FRASER STODDART

10.1 Introduction

Transistors [ref. 1] are solid state electronic devices capable of amplification and switching operations. By varying an input signal (current or voltage), they are switched reversibly between a *State 0* and a *State 1*. The two states differ in the magnitude of an output signal (current or voltage) that is amplified on going from *State 0* to *State 1*. By interconnecting appropriately several transistors, electronic circuits able to solve logic functions [ref. 2] can be fabricated. The complexity of a logic function and the speed at which it is carried out by an electronic circuit are related to the number of transistors integrated within the circuit. Thus, one of the major goals of the electronic industry is to build ultradensely integrated electronic circuits containing the largest possible number of transistors. This objective can only be achieved by reducing as much as possible the sizes of these switching devices. Indeed, over the past decades the dimensions of transistors have shrunk at an exponential rate and the smallest commercially available transistors have reached micrometer sizes. Stimulated by this tremendous pace toward miniaturization, a number of researchers have envisaged [ref. 3] the possibility of designing and fabricating molecular-sized electronic devices. In particular, bistable molecular and supramolecular [ref. 4] systems that can be switched [ref. 5] reversibly between a *State 0* and a *State 1* by using external control are expected to lead to a new generation of subnanometer-sized transistors ideal for the fabrication of ultradensely integrated electronic circuits and the computers of the future.

Molecules incorporating interlocked [refs. 6, 7] components (Fig. 10.1) and their supramolecular analogs are suitable candidates for the generation of bistable chemical systems. A [2]pseudorotaxane is a *supramolecular complex* composed of a macrocyclic host encircling a linear guest. The two components are held together solely by noncovalent bonding interactions and they can

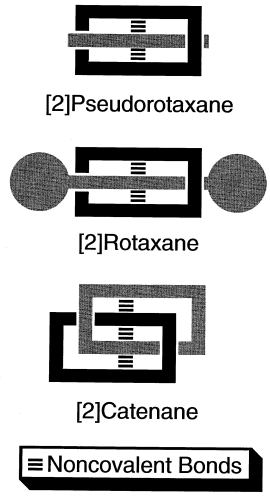

Figure 10.1. Schematic representations of a [2]pseudorotaxane, a [2]rotaxane, and a [2]catenane.

become dissociated from one another in solution. By contrast, bulky stoppers attached covalently to the termini of the linear component of a [2]rotaxane prevent dethreading. Similarly, the two interlocked macrocyclic components of a [2]catenane cannot dissociate from one another unless at least one covalent bond is cleaved. Thus, even although they are composed of two 'unbound' components, [2]rotaxanes and [2]catenanes behave as *single molecules*. These intriguing superstructural and structural features possessed by [2]pseudorotaxanes and by [2]rotaxanes and [2]catenanes, respectively, could pave the way for the realization of bistable systems. In many instances, the relative movements [ref. 8] of the interlocked components can be triggered by chemical, electrochemical, and photochemical stimuli (input signal) forcing the molecule or the complex to switch between two nondegenerate states (*State 0* and *State 1*) that can be distinguished spectroscopically (output signal).

10.2 [2]Pseudorotaxanes

The complexation/decomplexation of a linear guest by a macrocyclic host can be exploited [ref. 7] (Fig. 10.2) to switch reversibly between two states. When the two components are dissociated, the system is in its *State 0*. When they are associated in the form of a [2]pseudorotaxane, the system is in its *State 1*. Switching between these two states can be achieved [ref. 7] by protonation/deprotonation, by oxidation/reduction, or by photoinduced isomerization of the guest. Alternatively, the addition/removal of a sequestering agent able to

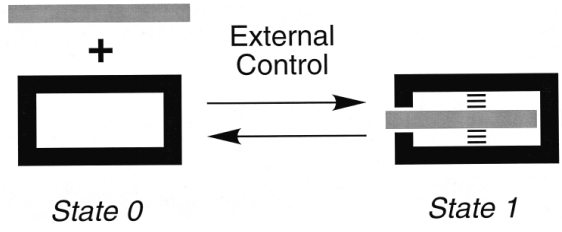

Figure 10.2. Externally controlled switching between a [2]pseudorotaxane (*State 1*) and its separate components (*State 0*).

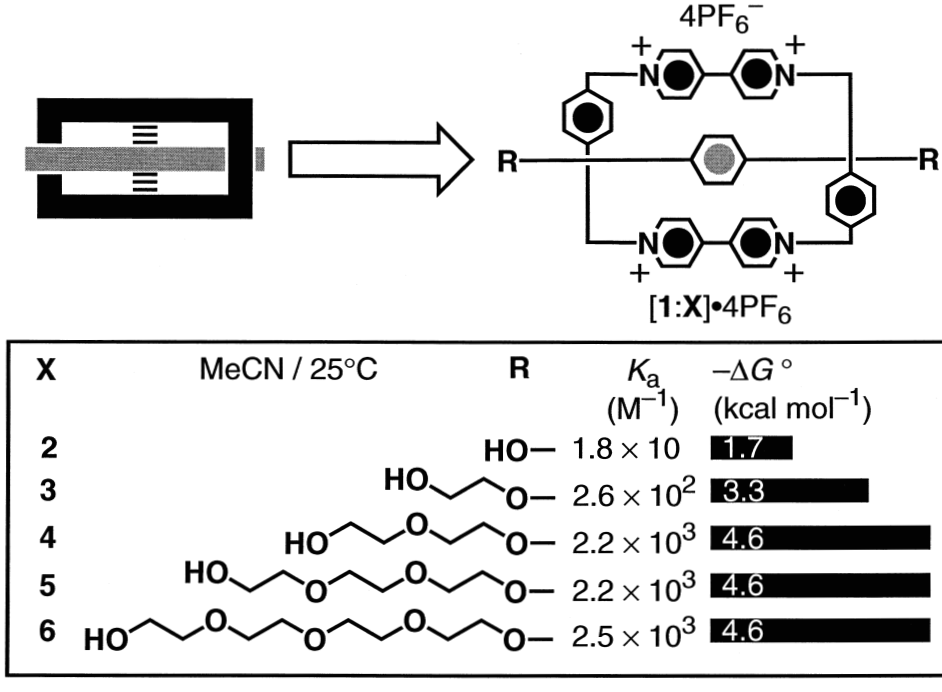

Figure 10.3. The [2]pseudorotaxanes [**1**:**2**]•4PF$_6$–[**1**:**6**]•4PF$_6$ and their association constants (K_a) and free energies of complexation ($-\Delta G°$) in MeCN at 25 °C.

form a strong adduct with the guest can be exploited [ref. 7] to switch the system between *State 0* and *State 1*. An ideal macrocyclic host for the realization of such bistable systems is the tetracationic cyclophane **1**•4PF$_6$ illustrated in Fig. 10.3. This host incorporates two dicationic bipyridinium recognition sites and is able to bind [refs. 9, 10] π-electron rich aromatic polyethers inside its cavity. The association constants (K_a) and the free energies of complexation ($-\Delta G°$) for the binding of the guests **2**–**6** reveal [refs. 9a, b] that the number of oxygen atoms incorporated in the substituents attached to the aromatic ring of the guest influences dramatically the binding event. The K_a value increases by one

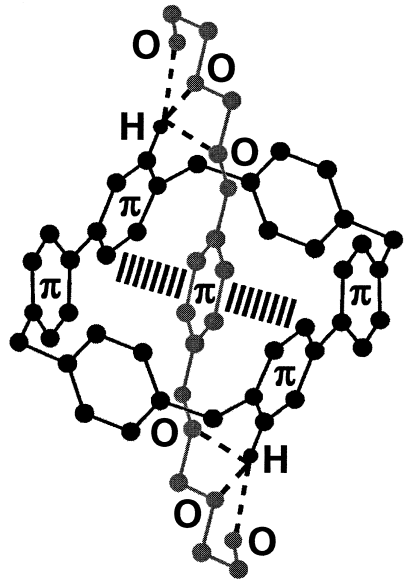

Figure 10.4. The geometry adopted by the [2]pseudorotaxane [**1**:**4**]$^{4+}$ in the solid state and the intercomponent [C–H···O] and [π···π] stacking interactions.

order of magnitude approximately on going from **2** to **3** and from **3** to **4**. Thereafter, however, it remains more or less constant on going from **4** to **5** and from **5** to **6**. These results indicate that the first three oxygen atoms are essential to the realization of strong binding between host and guest. Indeed, the solid state structure of the [2]pseudorotaxane [**1**:**4**]$^{4+}$ reveals [ref. 9b] (Fig. 10.4) intercomponent [C−H···O] interactions [ref. 11] between some of the bipyridinium hydrogen atoms in the α-position with respect to the nitrogen atoms and the three oxygen atoms of each polyether chain. These noncovalent bonding interactions are accompanied by [π···π] stacking [ref. 12] between the π-electron deficient bipyridinium units and the π-electron rich 1,4-dioxybenzene ring. When the π-electron density of the aromatic ring of the guest is reduced by attaching four (**7**) or two (**8**) electron withdrawing fluorine substituents, no or only weak complexation is detected [refs. 9c, e], respectively (Fig. 10.5). By contrast, when a 1,5-dioxynaphthalene recognition site (**9**) is incorporated in the guest a much stronger complex is formed [ref. 9d]. The remarkable stability of the complex [**1**:**9**]•4PF_6 was exploited [ref. 9d] to template [ref. 13] (Fig. 10.6) the formation of **1**•4PF_6 from its precursors. When **10**•2PF_6 and **11** are reacted under high pressure conditions in the presence of **9**, **1**•4PF_6 is obtained in a yield of 81%, after counterion exchange.

The host **1**•4PF_6 and the guest **12** form [ref. 14] (step 1 in Fig. 10.7) spontaneously the [2]pseudorotaxane [**1**:**12**]•4PF_6 when mixed in CD_3CN. Protonation

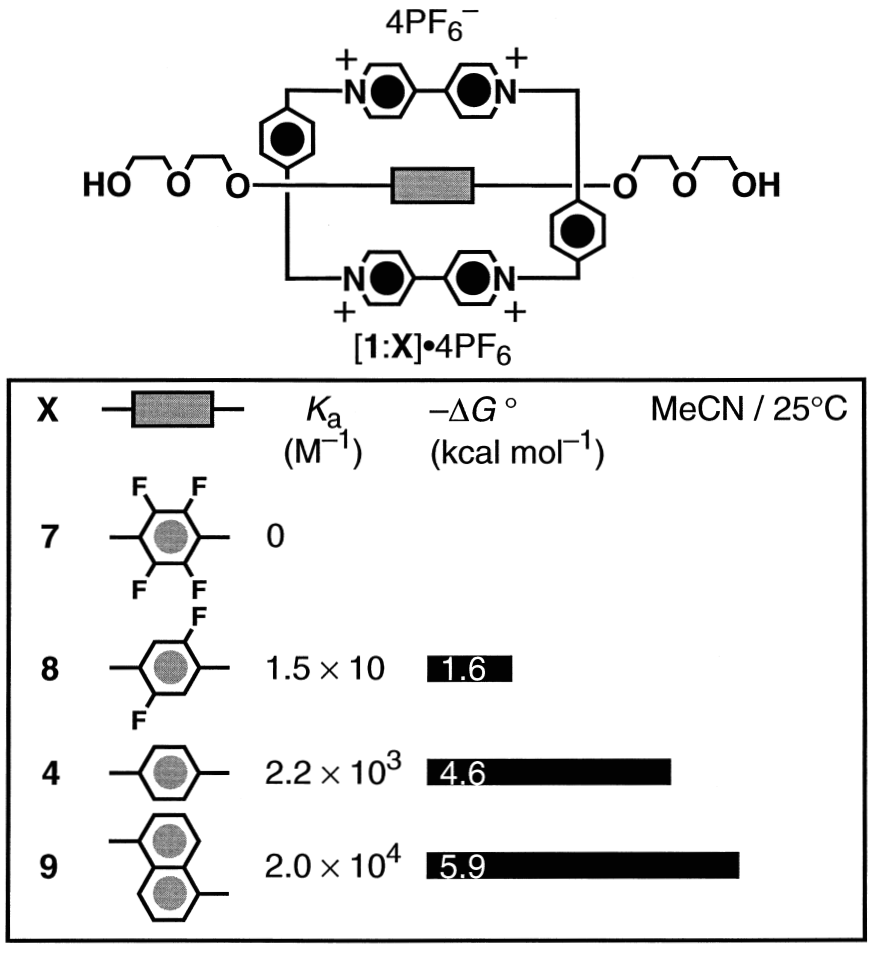

Figure 10.5. The [2]pseudorotaxanes [**1**:**4**]•4PF_6 and [**1**:**7**]•4PF_6–[**1**:**9**]•4PF_6 and their association constants (K_a) and free energies of complexation ($-\Delta G°$) in MeCN at 25 °C.

of the amino groups of the guest occurs after the addition (step 2 in Fig. 10.7) of CF_3CO_2H. The resulting dicationic guest is expelled (step 3 in Fig. 10.7) from the cavity of the tetracationic host as a result of electrostatic repulsion. Deprotonation of the ammonium centers of the guest occurs after the addition (step 4 in Fig. 10.7) of *i*-Pr_2NEt. The regenerated neutral form of the guest reinserts itself inside the cavity of the host, yielding (step 1 in Fig. 10.7) the original [2]pseudorotaxane [**1**:**12**]•4PF_6. As a result of [$\pi\cdots\pi$] stacking interactions between the π-electron deficient bipyridinium units and the π-electron rich 1,4-dioxybenzene ring, the occurrence of complexation and the decomplexation steps are accompanied by the appearance and disappearance, respectively, of the charge transfer band. As a result, the acid/base-controlled

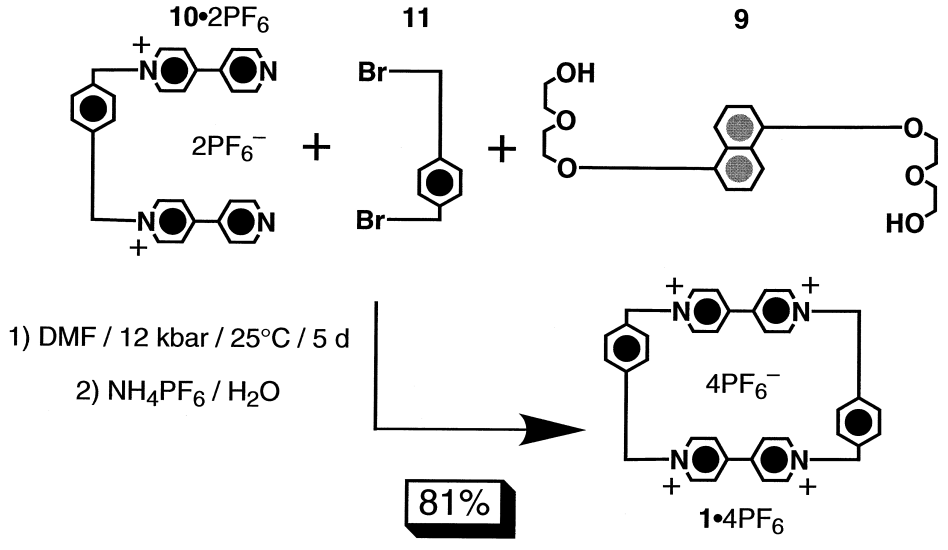

Figure 10.6. The template-directed synthesis of **1**•4PF_6.

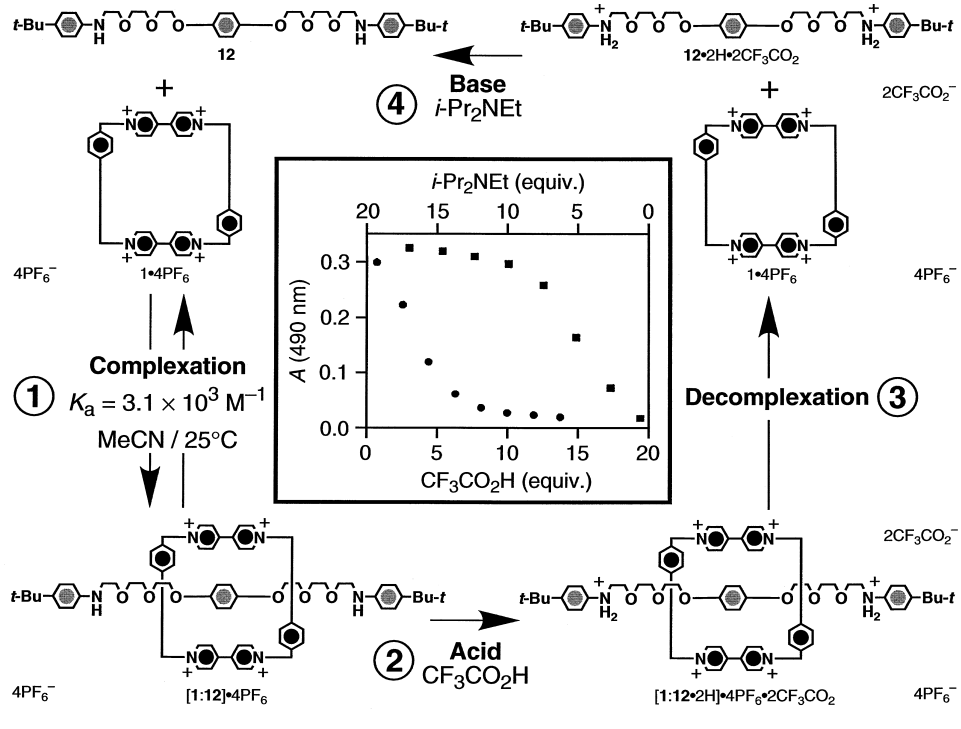

Figure 10.7. The acid/base-controlled switching of the [2]pseudorotaxane [**1**:**12**]•4PF_6 and the change in the absorbance (A) of the charge transfer band ($\lambda_{max} = 490$ nm) associated with [**1**:**12**]•4PF_6 upon addition of CF_3CO_2H and of i-Pr_2NEt is shown.

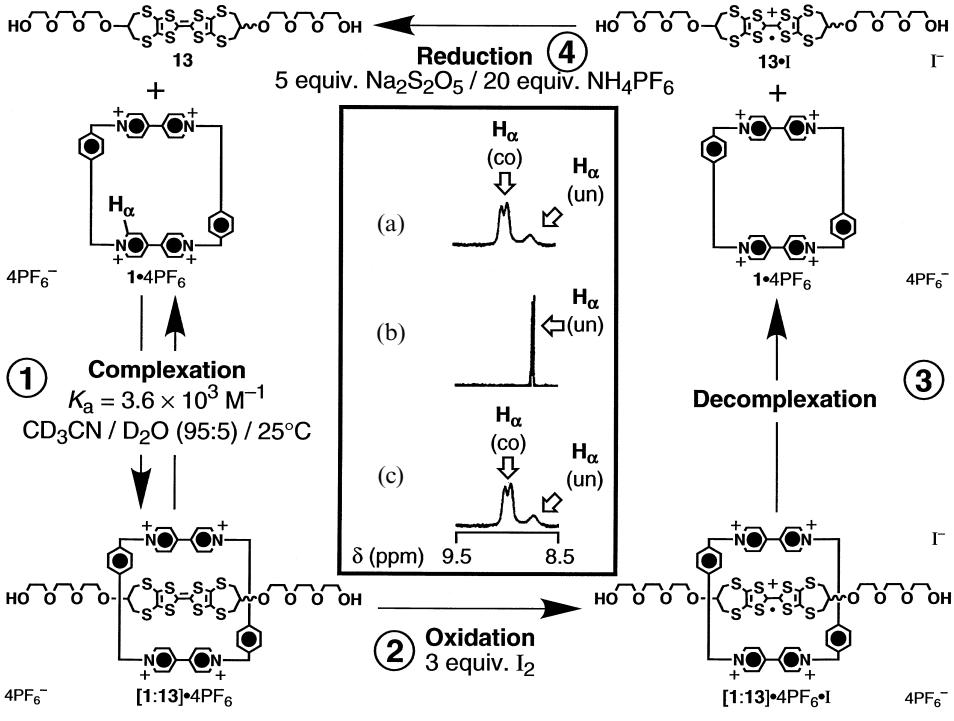

Figure 10.8. The redox-controlled switching of the [2]pseudorotaxane [**1**:**13**]•4PF_6 and the partial ^{1}H-NMR spectra [400 MHz, CD_3CN/D_2O (95:5), 25°C] of an equimolar mixture of **1**•4PF_6 and **13** (a) after complexation, (b) after oxidation and decomplexation, and (c) after reduction and complexation. The bipyridinium hydrogen atoms (H_α) in the α-positions with respect to the nitrogen atoms were used as the probe protons and (co) and (un) stand for complexed and uncomplexed species, respectively.

switching [ref. 15] of this system can be followed (inset in Fig. 10.7) by absorption spectroscopy. In the absence of CF_3CO_2H, a charge transfer band ($\lambda_{max} = 490$ nm) is observed. The gradual addition of CF_3CO_2H is accompanied by the decrease of the absorbance (A) associated with the charge transfer band as the guest is protonated and subsequently expelled from the cavity of the host. After the addition of *c.* 20 equivalents of CF_3CO_2H, no charge transfer band can be detected. The gradual addition of *i*-Pr_2NEt is accompanied by the increase of the A value as the guest is deprotonated and subsequently complexed by the host.

The host **1**•4PF_6 and the guest **13** form [ref. 16] (step 1 in Fig. 10.8) spontaneously the [2]pseudorotaxane [**1**:**13**]•4PF_6 when mixed in CD_3CN/D_2O (95:5). Oxidation of the tetrathiafulvalene unit of the guest occurs after the addition (step 2 in Fig. 10.8) of three equivalents of I_2. The resulting monocationic guest

is expelled (step 3 in Fig. 10.8) from the cavity of the tetracationic host as a result of electrostatic repulsion. Reduction of the tetrathiafulvalene unit of the guest occurs after the addition (step 4 in Fig. 10.8) of five equivalents of $Na_2S_2O_5$ and a large excess of NH_4PF_6. The regenerated neutral form of the guest reinserts itself inside the cavity of the host, yielding (step 1 in Fig. 10.8) the original [2]pseudorotaxane [**1**:**13**]•4PF_6. The redox-controlled switching [ref. 17] of this system can be followed (inset in Fig. 10.8) by ^{1}H-NMR spectroscopy using the bipyridinium hydrogen atoms (H_α) in the α-positions with respect to the nitrogen atoms as the probe protons. As the [2]pseudorotaxane [**1**:**13**]•4PF_6 and its separate components are in slow exchange on the ^{1}H-NMR timescale, the spectrum shows ((a) in the inset in Fig. 10.8) signals for the H_α protons associated with the complexed (co) and the uncomplexed (un) tetracationic cyclophane. After the oxidation of the guest, decomplexation occurs and only the signals for the complexed cyclophane can be observed ((b) in the inset in Fig. 10.8). Reduction of the guest is followed by complexation and the original signals for the complexed and the uncomplexed tetracationic cyclophane appear ((c) in the inset in Fig. 10.8) once again in the ^{1}H-NMR spectrum.

The *trans*-isomer (*trans*-**14**) of the guest **14** is bound [ref. 18] (step 1 in Fig. 10.9) by **1**•4PF_6 to form the [2]pseudorotaxane [**1**:*trans*-**14**]•4PF_6 in CD_3CN. By contrast, the *cis*-isomer (*cis*-**14**) of **14** is not complexed by **1**•4PF_6. Thus, when a solution of **1**•4PF_6 and *trans*-**14** is irradiated ($\lambda = 360$ nm) for 1 h, isomerization (step 2 in Fig. 10.9) of the free guest from *trans* to *cis* occurs. As a result, the equilibrium between the [2]pseudorotaxane [**1**:*trans*-**14**]•4PF_6 and its separate components is displaced in favor of the uncomplexed species. Further irradiation ($\lambda = 440$ nm) for 1 h induces the reisomerization (step 3 in Fig. 10.9) of the free guest from *cis* to *trans*, restoring the original equilibrium between the [2]pseudorotaxane [**1**:*trans*-**14**]•4PF_6 and its separate components. The light-controlled switching [ref. 19] of this system can be followed (inset in Fig. 10.9) by ^{1}H-NMR spectroscopy using the bipyridinium hydrogen atoms (H_α) in the α-positions with respect to the nitrogen atoms as the probe protons. The ^{1}H-NMR spectrum of a CD_3CN solution of **1**•4PF_6 and the *trans*-isomer of the guest **14** reveals ((a) in the inset in Fig. 10.9) signals for H_α in the complexed (co) and the uncomplexed (un) species which are undergoing slow exchange on the ^{1}H-NMR timescale. After the photoinduced isomerization of the free guest from *trans* to *cis*, the intensities of the signals associated with the H_α protons in the complexed species decrease ((b) in the inset in Fig. 10.9) relative to those of the complexed species. However, after the photoinduced re-isomerization of the free guest from the *cis*- to *trans*-isomer, the original ratio between the intensities of the signals for the H_α protons associated with the complexed and the uncomplexed species is restored ((c) in the inset in Fig. 10.9).

The host **1**•4PF_6 binds [ref. 20] (step 1 in Fig. 10.10) the guest **15** in CD_3CN to form the [2]pseudorotaxane [**1**:**15**]•4PF_6. Upon addition of two equivalents of the sequestering agent, *o*-chloroanil (**16**), the adduct [**15**:**16**] is formed (step 2 in Fig. 10.10). As the free guest **15** is removed from the equilibrium, the [2]pseudorotaxane [**1**:**15**]•4PF_6 dissociates completely into its separate components. Reduction of the sequestering agent **16** destroys (step 3 in Fig. 10.10) the adduct [**15**:**16**], releasing the guest **15** and restoring the original equilibrium between the [2]pseudorotaxane [**1**:**15**]•4PF_6 and its separate components. The supramolecularly controlled switching [ref. 21] of this system can be followed (inset in Fig. 10.10) by ^{1}H-NMR spectroscopy using the phenoxy hydrogen atoms (H_a) in the *ortho*-positions with respect to the *t*-butyl substituents as the probe protons. The ^{1}H-NMR spectrum of a CD_3CN solution of **1**•4PF_6 and **15** reveals ((a) in the inset in Fig. 10.10) signals for the H_α protons in the

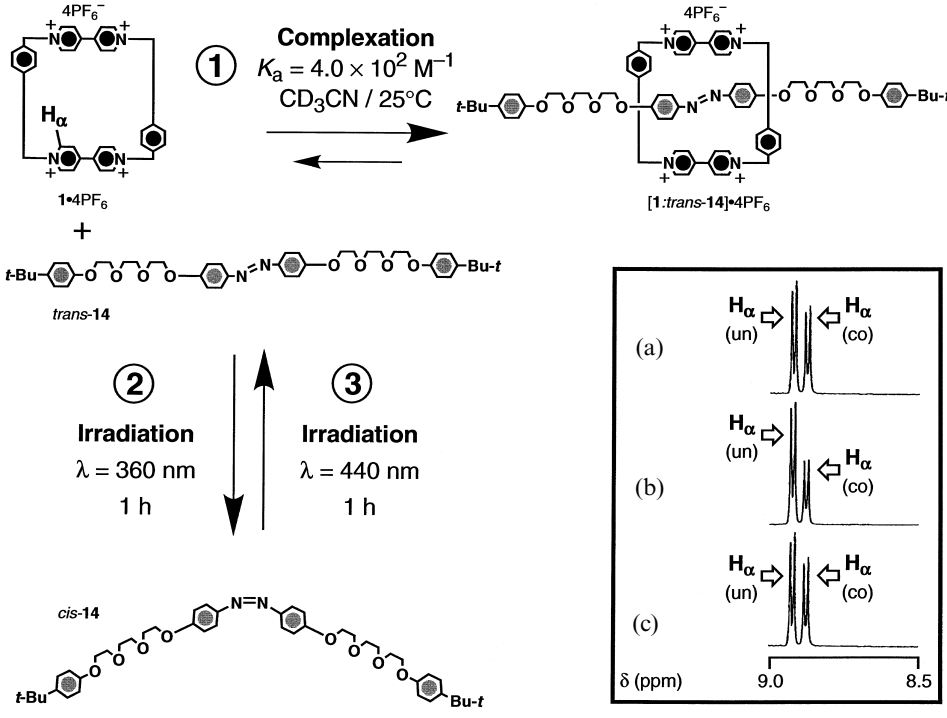

Figure 10.9. The light-controlled switching of the [2]pseudorotaxane [**1**:*trans*-**14**]•4PF_6 and the partial ^{1}H-NMR spectra [400 MHz, CD_3CN, 25 °C] of an equimolar mixture of **1**•4PF_6 and **14** (a) after complexation, (b) after irradiation ($\lambda = 360$ nm, 1 h) and decomplexation, and (c) after irradiation ($\lambda = 440$ nm, 1 h) and complexation. The bipyridinium hydrogen atoms (H_α) in the α-positions with respect to the nitrogen atoms were used as the probe protons and (co) and (un) stand for complexed and uncomplexed species, respectively.

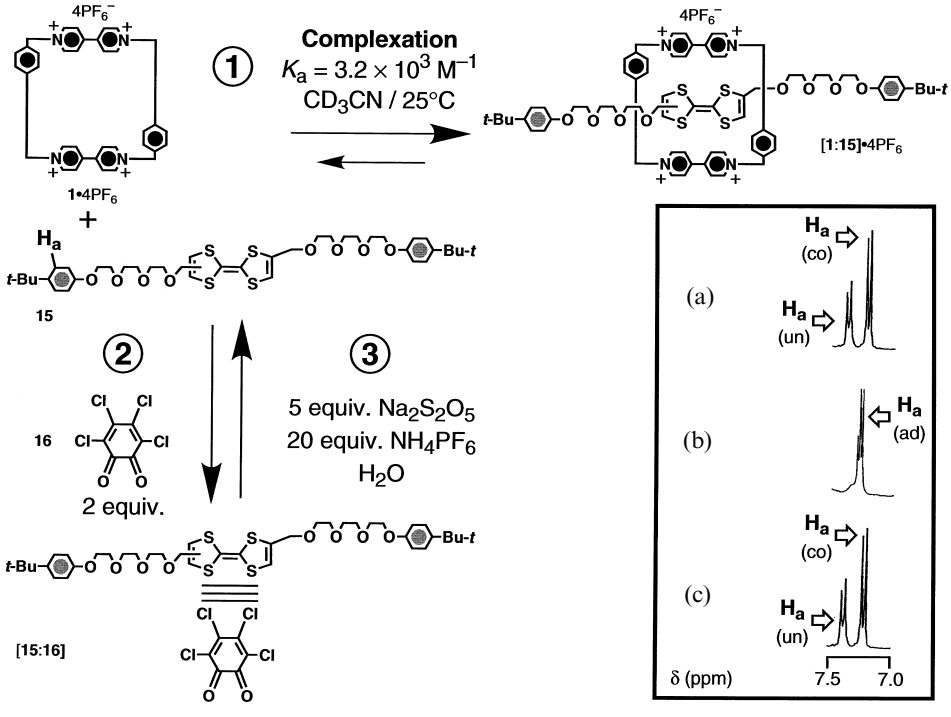

Figure 10.10. The supramolecularly controlled switching of the [2]pseudorotaxane [**1**:**15**]•4PF$_6$ and the partial ^{1}H-NMR spectra [400 MHz, CD_3CN, 25 °C] of an equimolar mixture of **1**•4PF$_6$ and **15** (a) after complexation, (b) after addition of **16**, and (c) after reduction of **16** are shown. The phenoxy hydrogen atoms (H_a) in the *ortho*-positions with respect to the *t*-butyl substituents as the probe protons and (co) and (un) stand for complexed and uncomplexed species, respectively.

complexed (co) and the uncomplexed (un) species which are in slow exchange on the ^{1}H-NMR timescale. After the addition of **16**, only the signals of the adduct [**15**:**16**] are observed ((b) in the inset in Fig. 10.10). However, after the reduction of **16** and release of the guest **15**, the ^{1}H-NMR spectrum shows ((c) in the inset in Fig. 10.10) the original signals for the H_α protons in the [2]pseudorotaxane [**1**:**15**]•4PF$_6$ and its separate components.

The redox-controlled switching between two [2]pseudorotaxanes was realized [ref. 22] (Fig. 10.11) using the host **1**•4PF$_6$ and the guests **9** and **17**. The 1,5-dioxynaphthalene-based guest **9** is fluorescent in its free form. Upon insertion of this guest inside the cavity of **1**•4PF$_6$ ($K_a = 10^5$ M^{-1} in H_2O at 25 °C), its fluorescence is quenched as a result of charge transfer interactions between the 1,5-dioxynaphthalene ring system and the sandwiching bipyridinium units. The binding of **17** by **1**•4PF$_6$ ($K_a \gg 10^5$ M^{-1} in H_2O at 25 °C) is accompanied by the appearance of a charge transfer band in the absorption spectrum as a result of

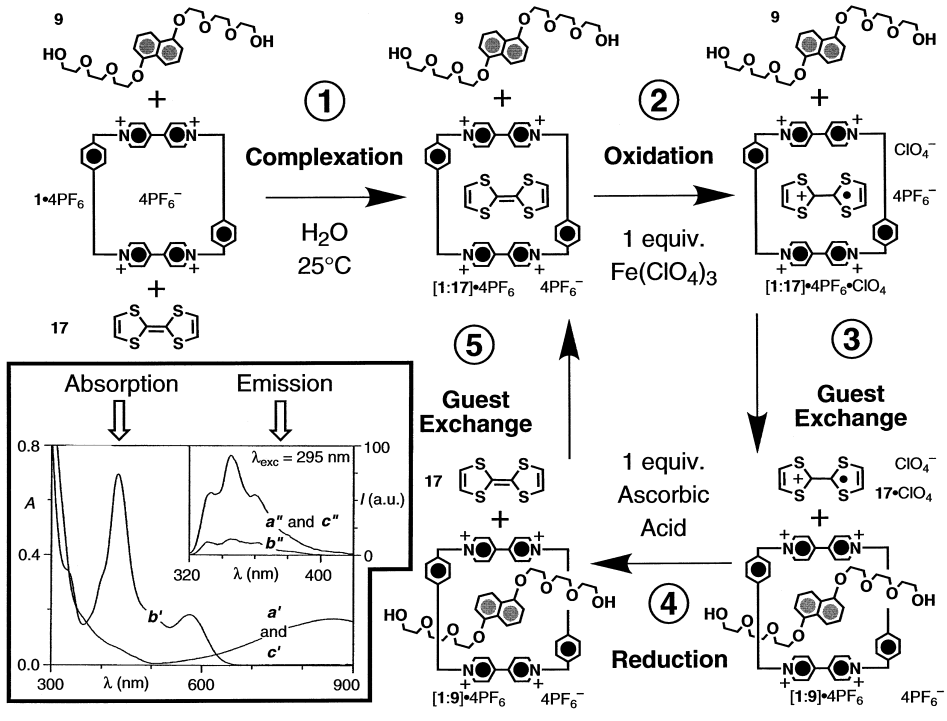

Figure 10.11. The redox-controlled switching between the [2]pseudorotaxanes [**1**:**9**]•4PF_6 and [**1**:**17**]•4PF_6 and the absorption and emission spectra of an equimolar mixture of **1**•4PF_6, **9**, and **17** (***a′/a″***) after the formation of [**1**:**17**]•4PF_6, (***b′/b″***) after oxidation and guest exchange, and (***c′/c″***) after reduction and guest exchange.

the [π · · · π] stacking interactions between the tetrathiafulvalene unit and the sandwiching bipyridinium units. Upon oxidation of the tetrathiafulvalene unit, the resulting monocationic guest is expelled from the cavity of the tetracationic host and the charge transfer band disappears. Thus, the complexation/decomplexation of the guests **9** and **17** by the host **1**•4PF_6 can be followed by emission and absorption spectroscopies, respectively. Upon mixing the host **1**•4PF_6 and the guests **9** and **17**, the [2]pseudorotaxane [**1**:**17**]•4PF_6 is formed (step 1 in Fig. 10.11) exclusively. The absorption and emission spectra show (***a′*** and ***a″*** in the inset in Fig. 10.11) respectively the charge transfer band (λ_{max} = 850 nm) of the complex [**1**:**17**]•4PF_6 and the fluorescence of the free guest **9**. After the addition of one equivalent of $Fe(ClO_4)_3$, **17** is oxidized (step 2 in Figure 10.11) to its radical cation $\mathbf{17}^{+\bullet}$ that is then expelled from the cavity of the tetracationic host and replaced (step 3 in Fig. 10.11) by the neutral guest **9**. As a result, the charge transfer band of the [2]pseudorotaxane [**1**:**17**]•4PF_6 disappears (***b′*** in the inset in Fig. 10.11) and is replaced by the characteristic absorption bands of the

radical monocation $\mathbf{17}^{+\bullet}$. Furthermore, the fluorescence of the 1,5-dioxynaphthalene ring system of **9** is quenched (***b″*** in the inset in Fig. 10.11) upon formation of the [2]pseudorotaxane [**1**:**9**]•$4PF_6$. Reduction (step 4 in Fig. 10.11) of $\mathbf{17}^{+\bullet}$ back to the neutral form **17** is followed (step 5 in Figure 10.11) by the exchange of the guests to yield the original [2]pseudorotaxane [**1**:**17**]•$4PF_6$. As a result, the charge transfer band of the complex [**1**:**17**]•$4PF_6$ and the fluorescence of the free guest **9** reappear (***c′*** and ***c′*** in the inset in Fig. 10.11).

The redox-controlled switching between two [2]pseudorotaxanes was also realized [ref. 12] (Fig. 10.12) using the hosts **1**•$4PF_6$ and **18** and the guest **17**. The redox potentials for the tetrathiafulvalene semicouples $\mathbf{17}^{+\bullet}/\mathbf{17}$ and $\mathbf{17}^{2+}/\mathbf{17}^{+\bullet}$ are +0.321 and +0.714 V, respectively, in MeCN. In the presence of the π-electron deficient host **1**•$4PF_6$, the redox potential of the semicouple $\mathbf{17}^{+\bullet}/\mathbf{17}$ shifts to +0.391 V while that of the semicouple $\mathbf{17}^{2+}/\mathbf{17}^{+\bullet}$ is unaffected. These observations indicate that only the neutral form of the guest **17** is bound by the host **1**•$4PF_6$ ($K_a = 10^5$ M^{-1} in MeCN at 25°C). In the presence of the π-electron rich host **18**, the redox potential of the semicouple $\mathbf{17}^{+\bullet}/\mathbf{17}$ is unaffected, while that of the semicouple $\mathbf{17}^{2+}/\mathbf{17}^{+\bullet}$ shifts to +0.700 V, suggesting that only the dicationic form $\mathbf{17}^{2+}$ is bound by **18** ($K_a = 4.1 \times 10^3$ M^{-1} in MeCN at 25°C). When the two hosts **1**•$4PF_6$ and **18** are mixed with the neutral

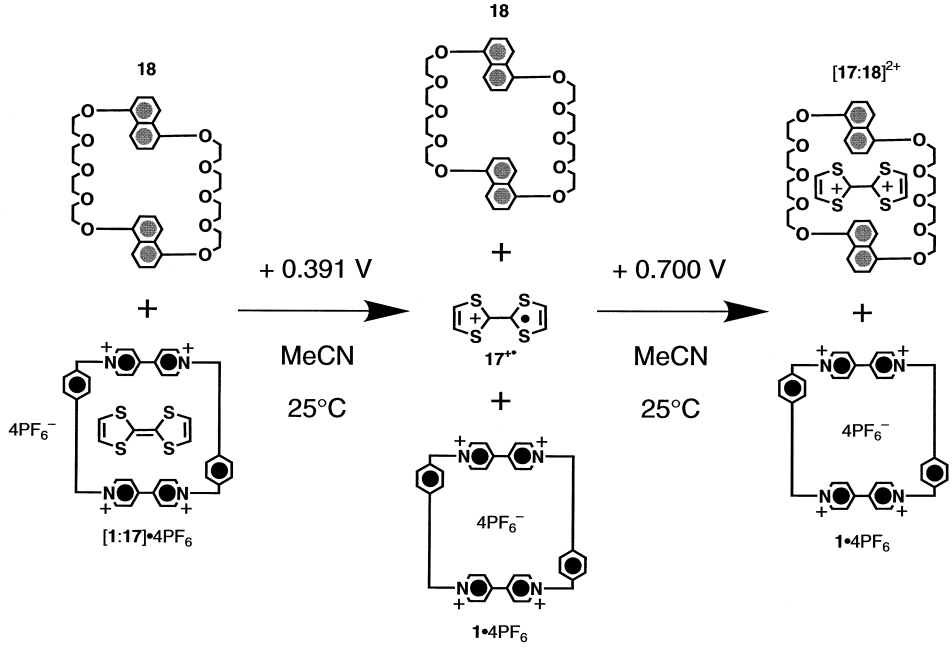

Figure 10.12. The redox-controlled switching between the [2]pseudorotaxanes [**1**:**17**]•$4PF_6$ and $[\mathbf{17}:\mathbf{18}]^{4+}$.

form **17** in MeCN, only the [2]pseudorotaxane [**1**:**17**]•4PF_6 is obtained. Oxidation (+0.391 V) of the guest **17** to the radical monocation $\mathbf{17}^{+\bullet}$ is accompanied by the dissociation of the complex. Further oxidation of $\mathbf{17}^{+\bullet}$ to the dication $\mathbf{17}^{2+}$ is followed by the formation of the [2]pseudorotaxane $[\mathbf{17}:\mathbf{18}]^{2+}$.

10.3 [2]Rotaxanes

The relative movement of the macrocyclic with respect to the dumbbell-shaped component of a [2]rotaxane can be exploited [ref. 7] (Fig. 10.13) to perform switching operations. Indeed, two states are associated with a [2]rotaxane incorporating two different recognition sites within its dumbbell-shaped component. The macrocyclic component encircles the recognition site *0* in *State 0*, while it is located around the recognition site *1* in *State 1*. Switching between these two states can be achieved [ref. 7] by protonation/deprotonation and/or by oxidation/reduction of one of the two recognition sites incorporated in the dumbbell-shaped component. A [2]rotaxane incorporating a π-electron deficient macrocyclic component and two π-electron rich recognition sites within its dumbbell-shaped component has been synthesized [ref. 24] as illustrated in Fig. 10.14. Reaction of **10**•2PF_6 and **11** in the presence of the dumbbell-shaped compound **19** gives the [2]rotaxane **20**•4PF_6 in a yield of 19%, after counterion exchange. At room temperature in CD_3CN, the 'shuttling' of the macrocyclic component from one π-electron rich recognition site to the other is fast on the ^{1}H-NMR timescale and averaged signals for probe protons in the two translational isomers associated with **20**•4PF_6 are observed in the ^{1}H-NMR spectrum. At −40 °C, this dynamic process becomes slow on the ^{1}H-NMR timescale and separate signals for the probe protons in the two translational isomers can be distinguished in a ratio of 84:16 in favor of the one having the more π-electron rich

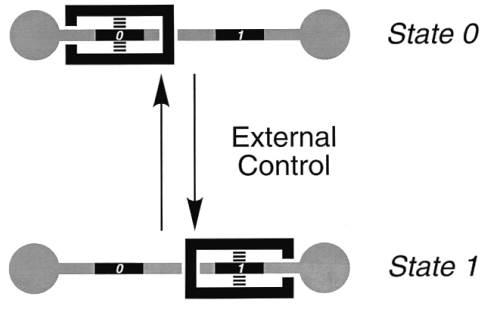

Figure 10.13. Externally controlled switching between the two states (*State 0* and *State 1*) associated with a [2]rotaxane incorporating two different recognition sites within the linear portion of its dumbbell-shaped component.

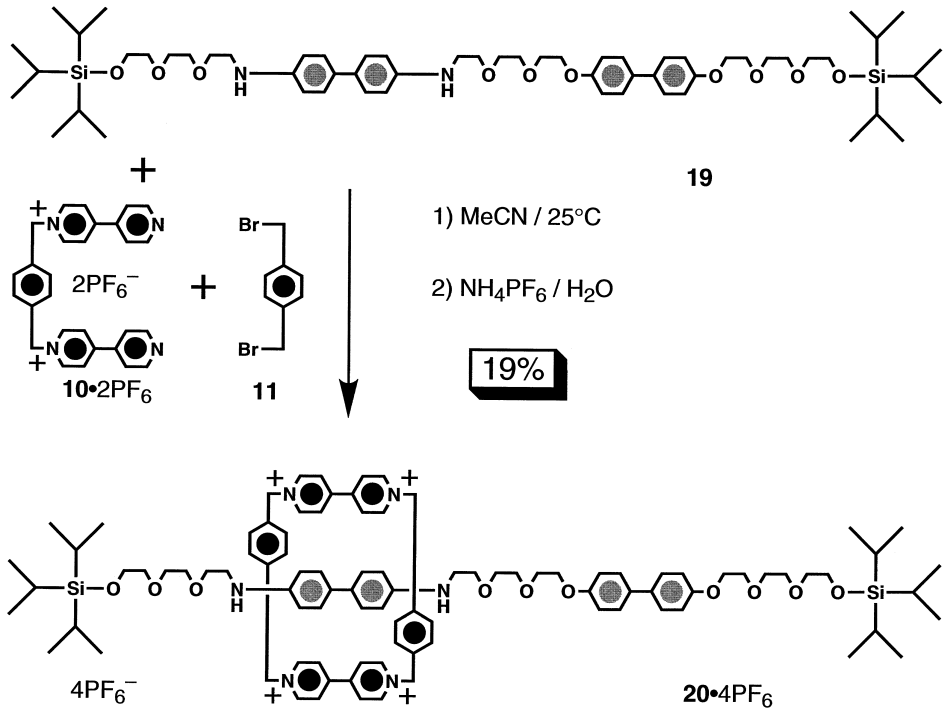

Figure 10.14. The template-directed synthesis of the [2]rotaxane **20**•4PF$_6$.

benzidine recognition site encircled by the tetracationic cyclophane component. Consistently, the absorption spectrum of **20**•4PF$_6$ reveals (***a*** in the inset in Fig. 10.15) an absorption band ($\lambda_{max} = 690$ nm) characteristic of charge transfer interactions between a benzidine unit and two sandwiching bipyridinium units. Upon addition of CF_3CO_2H, the nitrogen atoms of the benzidine recognition site become protonated (step 1 in Fig. 10.15). Electrostatic repulsion between the newly formed dicationic unit and the tetracationic cyclophane force the macrocyclic component to 'shuttle' (step 2 in Fig. 10.15) to the biphenol recognition site. As a result, the absorption band associated with the charge transfer interactions between the benzidine ring system and the bipyridinium units in the tetracationic cyclophane disappears (***b*** in the inset in Fig. 10.15). After the addition of C_5D_5N, deprotonation occurs (step 3 in Fig. 10.15) and the original equilibrium between the two translational isomers of **20**•4PF$_6$ is restored (step 4 in Fig. 10.15). Consistently, the absorption spectrum reveals (***c*** in the inset in Fig. 10.15) once again the charge transfer band associated with the interactions between the benzidine ring system and the bipyridinium units. Switching [ref. 25] of the [2]rotaxane **20**•4PF$_6$ can also be performed (Fig. 10.16) electrochemically by oxidizing/reducing the

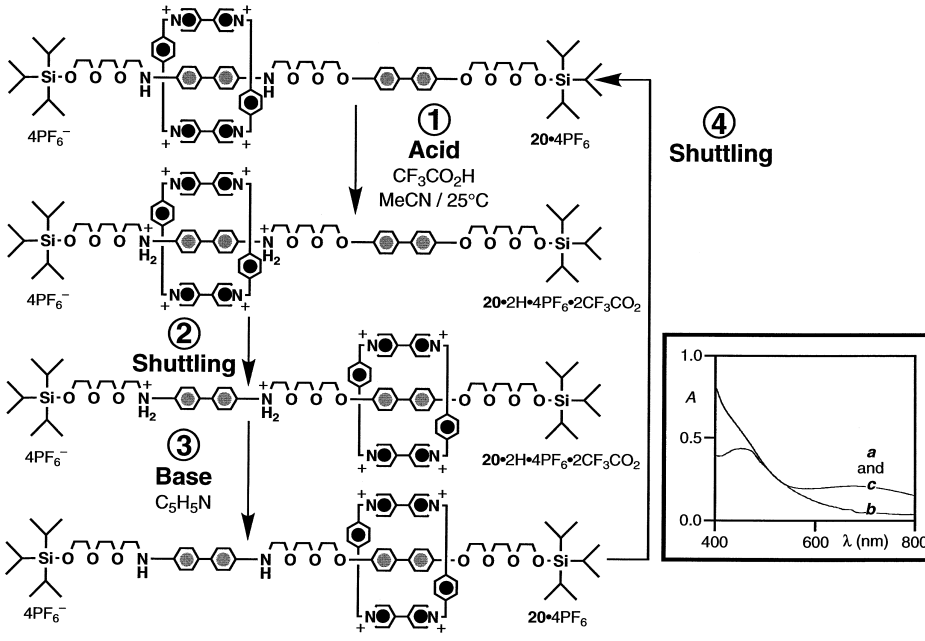

Figure 10.15. The acid/base-controlled switching of the [2]rotaxane **20**•4PF_6 and the absorption spectra (MeCN, 25 °C) of **20**•4PF_6 (***a***) before the addition of CF_3CO_2H, (***b***) after the addition of CF_3CO_2H and shuttling, and (***c***) after the addition of C_5H_5N and shuttling.

benzidine recognition site. The oxidation (step 1 in Fig. 10.16) of the benzidine unit to a radical cation forces the tetracationic cyclophane to 'shuttle' (step 2 in Fig. 10.16) to the biphenol recognition site as a result of electrostatic repulsion between the two positively-charged entities. Reduction (step 3 in Fig. 10.16) of the radical cation back to the neutral species restores (step 4 in Fig. 10.16) the original equilibrium between the two translational isomers of the [2]rotaxane **20**•4PF_6.

An alternative synthetic approach [ref. 26] to a [2]rotaxane incorporating two different recognition sites within the linear portion of its dumbbell-shaped component is illustrated in Fig. 10.17. Reaction of **21**•2PF_6 with **22** in the presence of the crown ether host **23** gives the [2]rotaxane **24**•3PF_6 in a yield of 38%, after counterion exchange. In $(CD_3)_2CO$ at 25 °C, the ^{1}H-NMR spectrum of the [2]rotaxane **24**•3PF_6 shows the selective binding of the ammonium recognition site by the macrocyclic polyether. This co-conformation [ref. 27] is stabilized by a combination of [$^+$N−H · · · O] and [C−H · · · O] hydrogen bonds between the acidic hydrogen atoms of the secondary dialkylammonium recognition site and the polyether oxygen atoms. Irradiation of the protons in positions 2 and 6 on the 3,5-di-*t*-butylbenzyl ring of the stopper adjacent to the

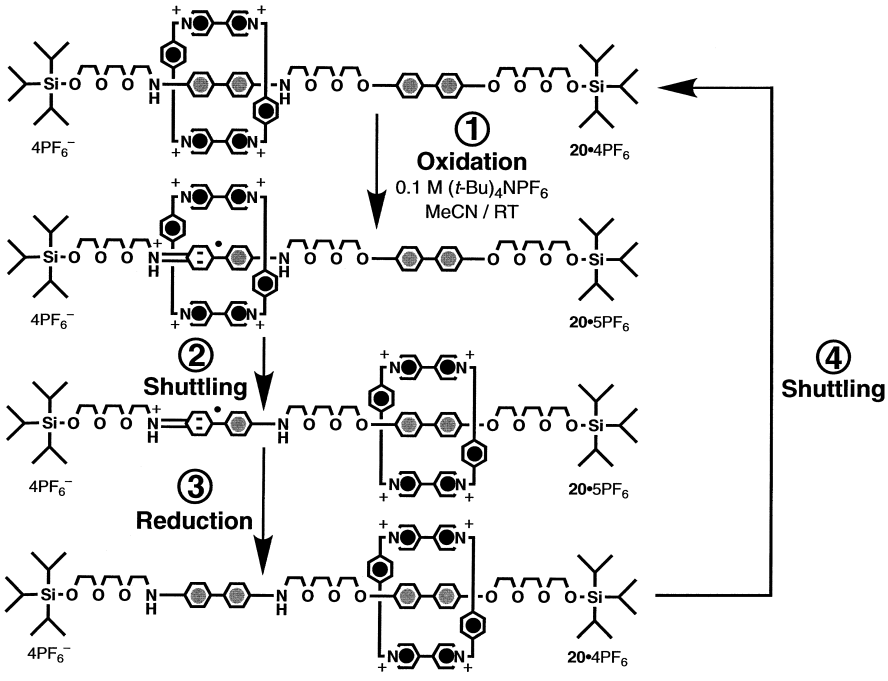

Figure 10.16. The redox-controlled switching of the [2]rotaxane **20**•4PF_6.

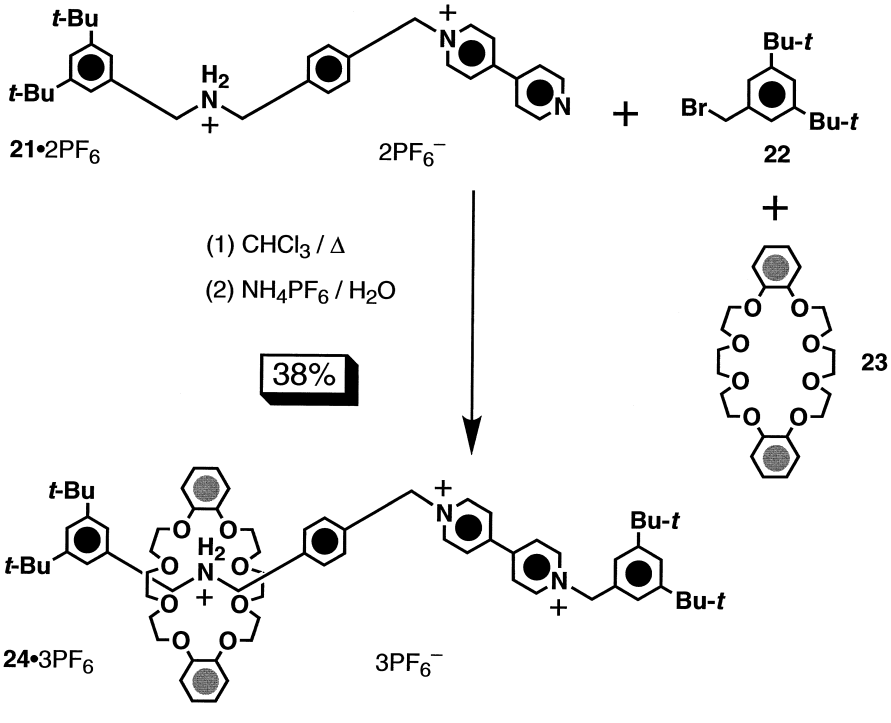

Figure 10.17. The template-directed synthesis of the [2]rotaxane **24**•3PF_6.

ammonium recognition site shows NOE enhancements of some of the resonances associated with the *O*-methylene protons in the crown ether. Addition of *i*-Pr_2NEt deprotonates (step 1 in Fig. 10.18) the ammonium recognition site. As a result, the macrocyclic polyether component 'shuttles' (step 2 in Fig. 10.18) to embrace one of the pyridinium rings of the bipyridinium recognition site. This step is accompanied by the appearance of a red color associated with charge transfer interactions between the pyridinium ring and the sandwiching catechol rings. Addition of CF_3CO_2H regenerates (step 3 in Fig. 10.18) the ammonium recognition site. Thus, the macrocyclic component 'shuttles' (step 4 in Fig. 10.18) back to encircle this $^+NH_2$ center and the orange color associated with the charge transfer interaction disappears. The acid/base-controlled switching of the [2]rotaxane **24**•$3PF_6$ can be followed (inset in Fig.10.18) by ^{1}H-NMR spectroscopy using the bipyridinium hydrogen atoms ($H_\beta{}^1$ and $H_\beta{}^2$) in the β-positions with respect to the nitrogen atoms as the probe protons. These protons give rise ((a) in the inset in Fig. 10.18) to one set of signals only in the

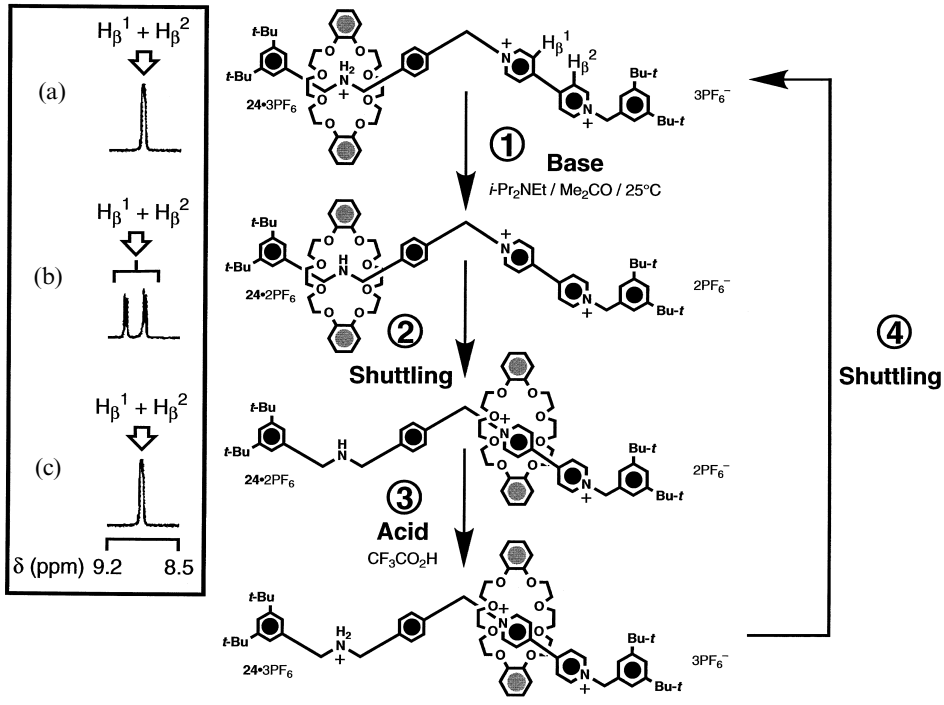

Figure 10.18. The acid/base-controlled switching of the [2]rotaxane **24**•$3PF_6$ and the partial ^{1}H-NMR spectra [400 MHz, $(CD_3)_2CO$, 25 °C] of **24**•$3PF_6$ (a) before the addition of *i*-Pr_2NEt, (b) after the addition of *i*-Pr_2NEt and shuttling, and (c) after the addition of CF_3CO_2H. The bipyridinium hydrogen atoms ($H_\beta{}^1$ and $H_\beta{}^2$) in the β-positions with respect to the nitrogen atoms were used as the probe protons.

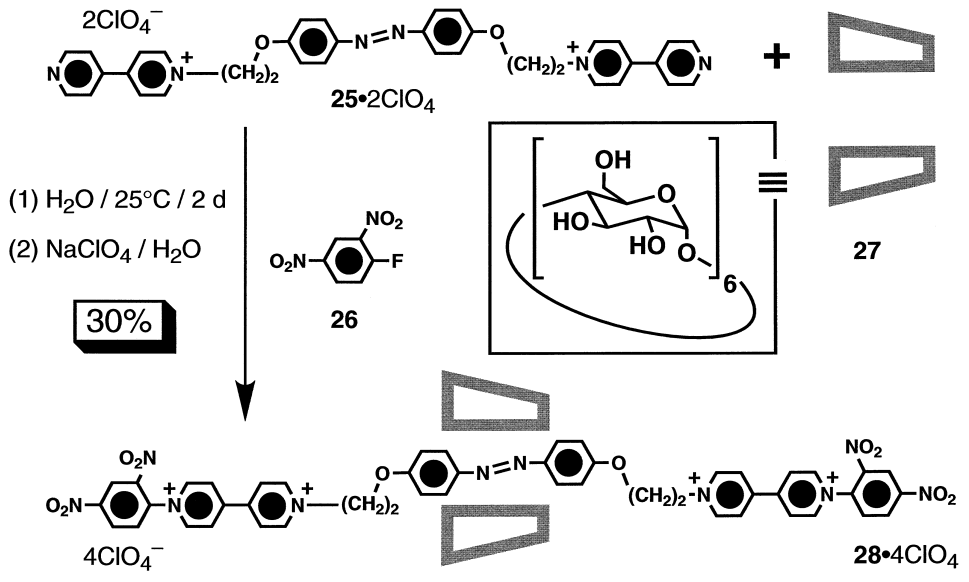

Figure 10.19. The template-directed synthesis of the [2]rotaxane **28**•4ClO_4.

^{1}H-NMR spectrum of the [2]rotaxane **24**•3PF_6 recorded in CD_3CN at 25°C. After the addition of *i*-Pr_2NEt and the 'shuttling' of the macrocyclic component to the bipyridinium recognition site, two distinct sets of signals are observed ((b) in the inset in Fig. 10.18) for $H_\beta{}^1$ and $H_\beta{}^2$. After the addition of CF_3CO_2H and the 'shuttling' of the macrocyclic component back to the ammonium recognition site, once again one set of signals is observed ((c) in the inset in Fig. 10.18) for $H_\beta{}^1$ and $H_\beta{}^2$.

The synthesis [ref. 28] of a [2]rotaxane incorporating a photoactive azobenzene unit in the linear portion of its dumbbell-shaped component is illustrated in Fig. 10.19. Reaction of **25**•2ClO_4 with **26** in the presence of α-cyclodextrin (**27**) gives the [2]rotaxane **28**•4ClO_4 in a yield of 30% after counterion exchange. In this [2]rotaxane, the cyclodextrin component encircles preferentially the *trans*-azobiphenoxy unit. However, upon irradiation ($\lambda = 360$ nm) of an aqueous solution of **28**•4ClO_4, isomerization (step 1 in Fig. 10.20) of the azobiphenoxy unit from *trans* to *cis* occurs. As a result, the macrocyclic component moves to encircle the bismethylene spacer bridging the *cis*-azobiphenoxy unit and one of the two bipyridinium units. Upon further irradiation ($\lambda = 430$ nm), the isomerization (step 2 in Fig. 10.20) of azobiphenoxy unit from *cis* back to *trans* occurs and is accompanied by the 'shuttling' of the cyclodextrin component back to the *trans*-azobiphenoxy unit. The light-controlled switching [ref. 29] of the [2]rotaxane **28**•4ClO_4 can be followed by circular dichroism measurements. Before irradiation, a positive circular dichroism induced band

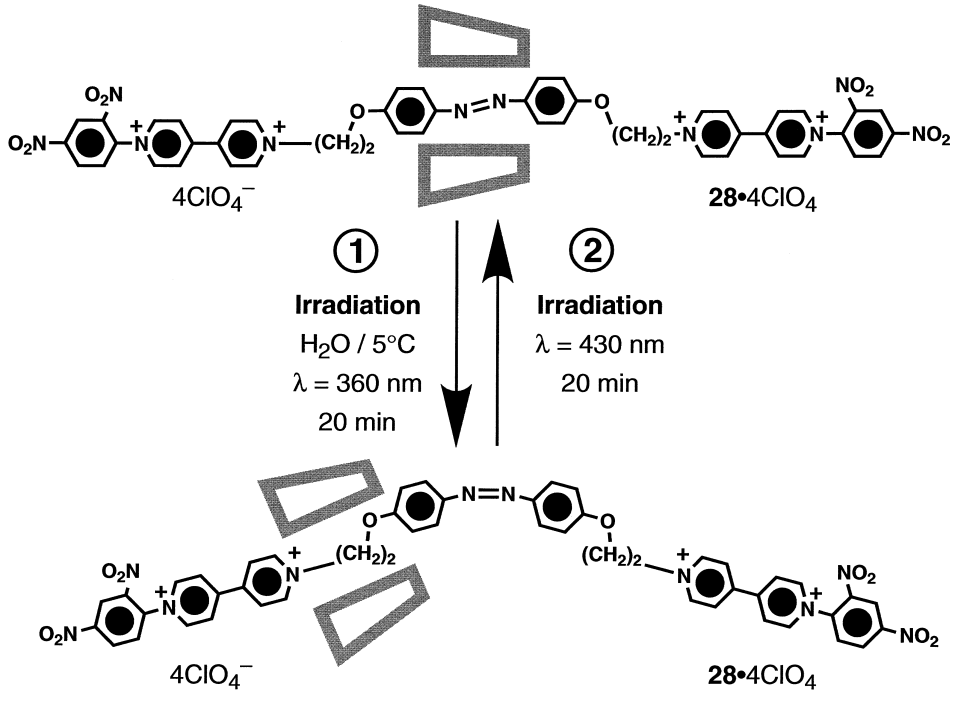

Figure 10.20. The light-controlled switching of the [2]rotaxane **28**•4ClO_4.

($\lambda = 360$ nm), corresponding to the π–π^* transition associated with the azobiphenoxy unit, is observed. After irradiation ($\lambda = 360$ nm), the intensity of this band decreases but is restored after irradiation at a longer wavelength ($\lambda = 430$ nm). Since the sign of a π–π^* transition associated with a guest encircled by an α-cyclodextrin is positive, the observed results indicate that the azobiphenoxy unit is inserted originally inside the cyclodextrin cavity and that it is expelled after irradiation at a wavelength of 360 nm.

10.4 [2]Catenanes

The circumrotation of one of the two macrocyclic components of a [2]catenane through the cavity of the other can be exploited [ref. 7] (Fig. 10.21) to perform switching operations. Indeed, two states are associated with a [2]catenane incorporating two different recognition sites within one of its two macrocyclic components. In *State 0*, the recognition site *0* comprised within one macrocyclic component is located inside the cavity of the other and the recognition site *1* is 'alongside'. In *State 1*, the recognition site *1* is 'inside' and the recognition site *0* is 'alongside'. Switching between these two states can be achieved [ref. 7]

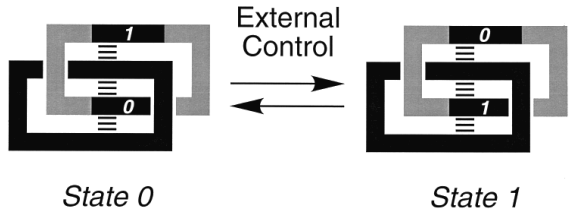

Figure 10.21. Externally controlled switching between the two states (*State 0* and *State 1*) associated with a [2]catenane incorporating two different recognition sites within one of its two macrocyclic components.

by oxidation/reduction of the recognition site *0* or *1* or by the addition/removal of a 'locking' component. [2]Catenanes incorporating a π-electron deficient macrocyclic component and two π-electron rich recognition sites within the second macrocycle can be synthesized [refs. 20, 30] as illustrated in Fig. 10.22. Reaction of **10**•2PF_6 and **11** in the presence of either **29** or **30** gives the [2]catenanes **31**•4PF_6 or **32**•4PF_6, respectively, in yields of 43 or 23%, respectively, after counterion exchange. The X-ray crystallographic analysis of the [2]catenane **32**•4PF_6 reveals (Fig. 10.23) that the tetrathiafulvalene recognition site is located exclusively inside the cavity of the tetracationic cyclophane in the solid state, while the 1,5-dioxynaphthalene recognition site is positioned alongside. In both [2]catenanes, absorption and ^{1}H-NMR spectroscopic studies show (*vide infra*) that the tetrathiafulvalene unit is also located preferentially 'inside' in solution. This selectivity offers the possibility of switching these [2]catenanes by oxidation/reduction of their tetrathiafulvalene units. In the case of **31**•4PF_6, oxidation of the tetrathiafulvalene unit is achieved (step 1 in Fig. 10.24) upon addition of one equivalent of $Fe(ClO_4)_3$. The resulting monocationic unit is expelled from the cavity of the tetracationic cyclophane and it is replaced (step 2 in Fig. 10.24) by the neutral 1,4-dioxybenzene recognition site. Upon addition of one equivalent of $Na_2S_2O_5$ and H_2O, the tetrathiafulvalene unit is reduced (step 3 in Fig. 10.24) back to its neutral state. Circumrotation of the macrocyclic polyether through the cavity of the tetracationic cyclophane follows (step 4 in Fig. 10.24) immediately, resulting in the reinsertion of the tetrathiafulvalene recognition site inside the cavity of the π-electron deficient macrocycle. The redox-controlled switching [ref. 31] of the [2]catenane **31**•4PF_6 can be monitored (inset in Fig. 10.24) by absorption spectroscopy. Initially, an absorption band ($\lambda_{max} = 850$ nm) associated with charge transfer interactions between the tetrathiafulvalene unit and the sandwiching bipyridinium units is observed (***a*** in the inset in Fig. 10.24). After oxidation of the tetrathiafulvalene unit and circumrotation of the macrocyclic polyether, the charge transfer band disappears (***b*** in the inset in Fig. 10.24) and is replaced by the characteristic

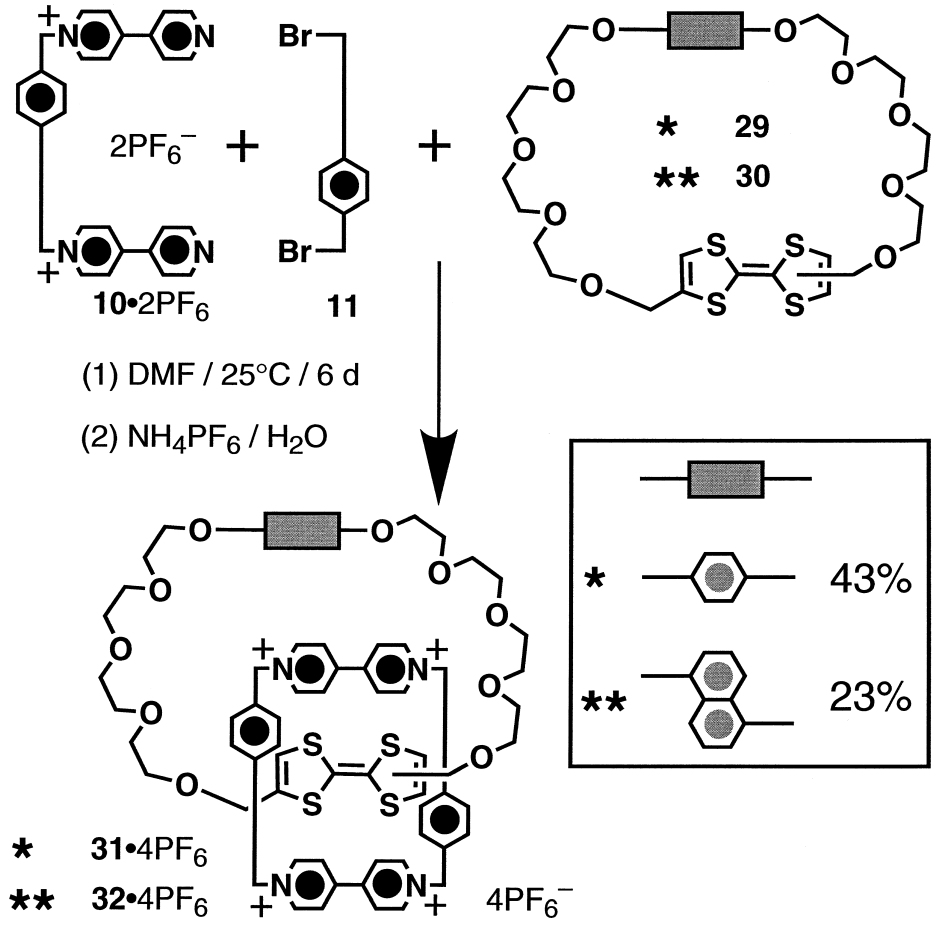

Figure 10.22. The template-directed synthesis of the [2]catenanes **31**•4PF$_6$ and **32**•4PF$_6$.

absorption bands of the monocationic form of tetrathiafulvalene. After reduction of the tetrathiafulvalene unit back to its neutral form and circumrotation of the macrocyclic polyether, the original charge transfer band is restored (***c*** in the inset in Fig. 10.24). The [2]catenane **31**•4PF$_6$ can be also switched by supramolecular control. In CD_3CN at 25 °C, two translational isomers in equilibrium are associated (step 1 in Fig. 10.25) with the [2]catenane **31**•4PF$_6$. The major translational isomer incorporates the tetrathiafulvalene recognition site 'inside' and the 1,4-dioxybenzene ring 'alongside'. The minor translational isomer incorporates the 1,4-dioxybenzene recognition site 'inside' and the tetrathiafulvalene unit 'alongside'. Upon addition of two equivalents of *o*-chloroanil (**16**), the equilibrium between the two translational isomers of

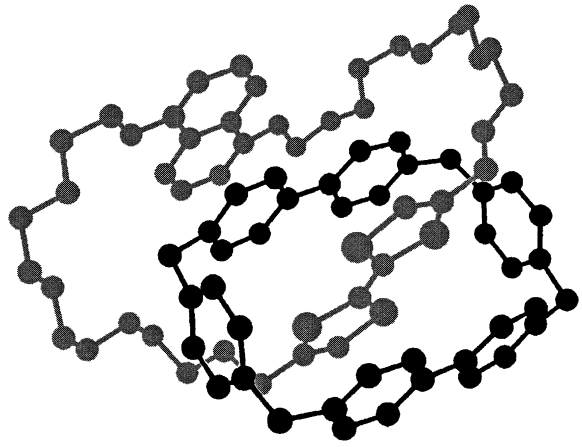

Figure 10.23. The geometry adopted by the [2]catenane $\mathbf{32}^{4+}$ in the solid state.

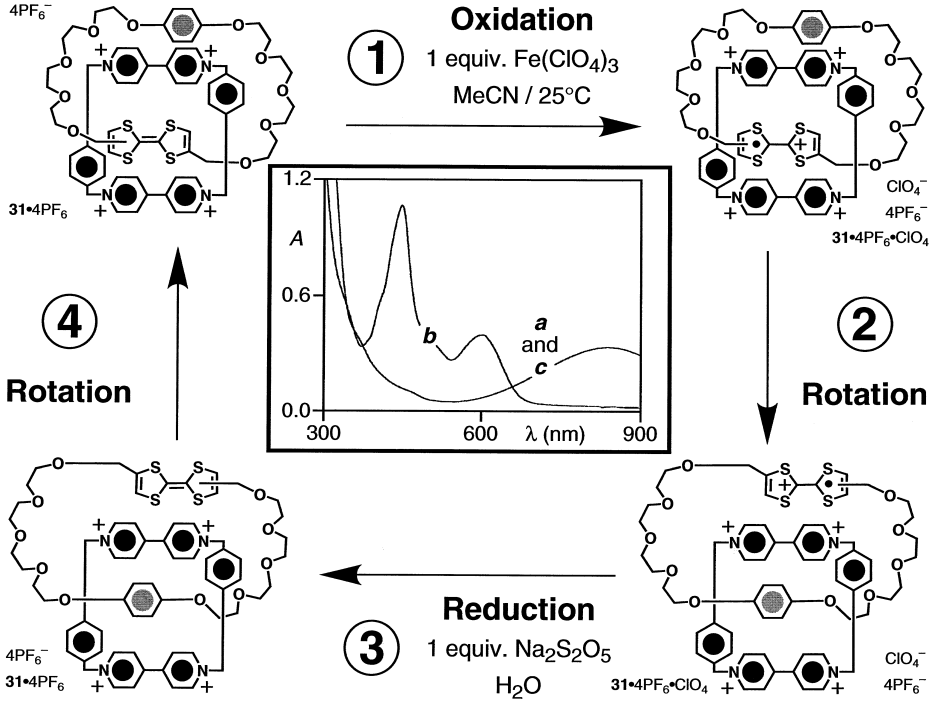

Figure 10.24. The redox-controlled switching of the [2]catenane **31**•4PF_6 and the absorption spectra (MeCN, 25°C) of **31**•4PF_6 (***a***) before oxidation, (***b***) after oxidation and rotation, and (***c***) after reduction and rotation.

31•4PF_6 is displaced completely in favor of the one incorporating the 1,4-dioxybenzene recognition site 'inside'. Indeed, the tetrathiafulvalene unit is 'locked' (step 2 in Fig. 10.25) 'alongside' by [π···π] stacking interactions with the *o*-chloroanil unit to form the adduct [**16**:**31**]•4PF_6. Upon addition of five equivalents of $Na_2S_2O_5$ and a large excess of NH_4PF_6/H_2O, the *o*-chloroanil unit is reduced, the adduct is destroyed (step 3 in Fig. 10.25), and the original equilibrium between the two translational isomers of the [2]catenane **31**•4PF_6 is restored. The supramolecularly controlled switching of the [2]catenane **31**•4PF_6 can be monitored (inset in Fig. 10.25) by ^{1}H-NMR spectroscopy using the tetrathiafulvalene and the 1,4-dioxybenzene hydrogen atoms (H_b and H_c) as the probe protons. As a result of the presence of the *cis* and the *trans* forms (Fig. 10.25) of the tetrathiafulvalene unit, the ^{1}H-NMR spectrum (CD_3CN, 25 °C) of the [2]catenane **31**•4PF_6 shows ((a) in the inset in Fig. 10.25) two singlets of different intensities for H_b and two more for H_c. Upon addition of **16**, the relative intensities of the two singlets for H_b change ((b) in the inset in Fig.

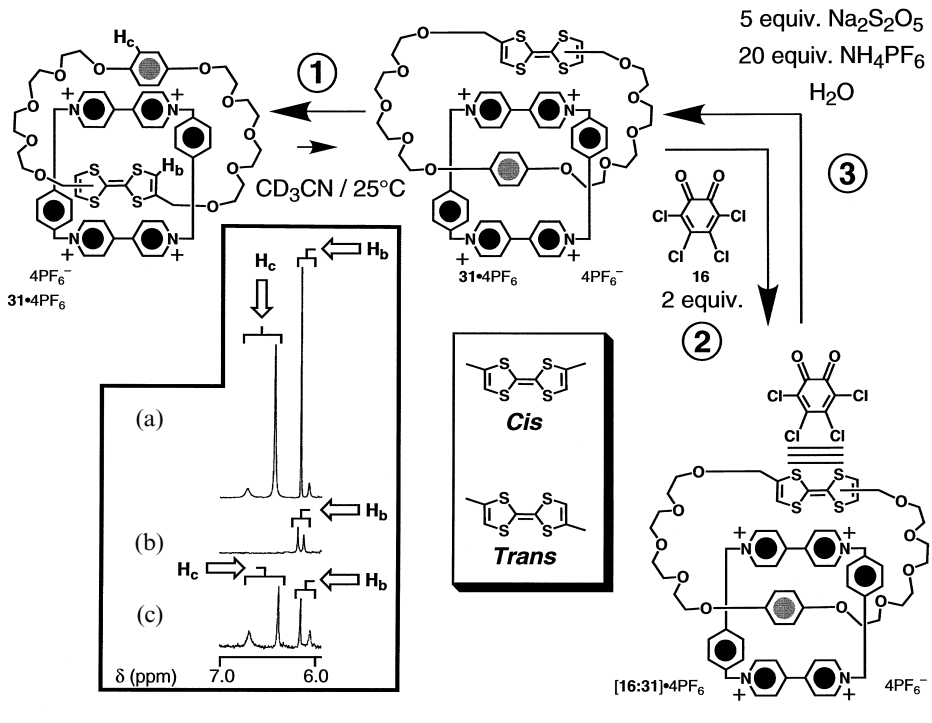

Figure 10.25. The supramolecularly controlled switching of the [2]catenane **31**•4PF_6 and the partial ^{1}H-NMR spectra (400 MHz, CD_3CN, 25 °C) of **31**•4PF_6 (a) before the addition of **16**, (b) after the addition of **16** and the formation of [**16**:**31**]•4PF_6, and (c) after the reduction of **16** and rotation. The tetrathiafulvalene and the 1,4-dioxybenzene hydrogen atoms (H_b and H_c) were used as the probe protons.

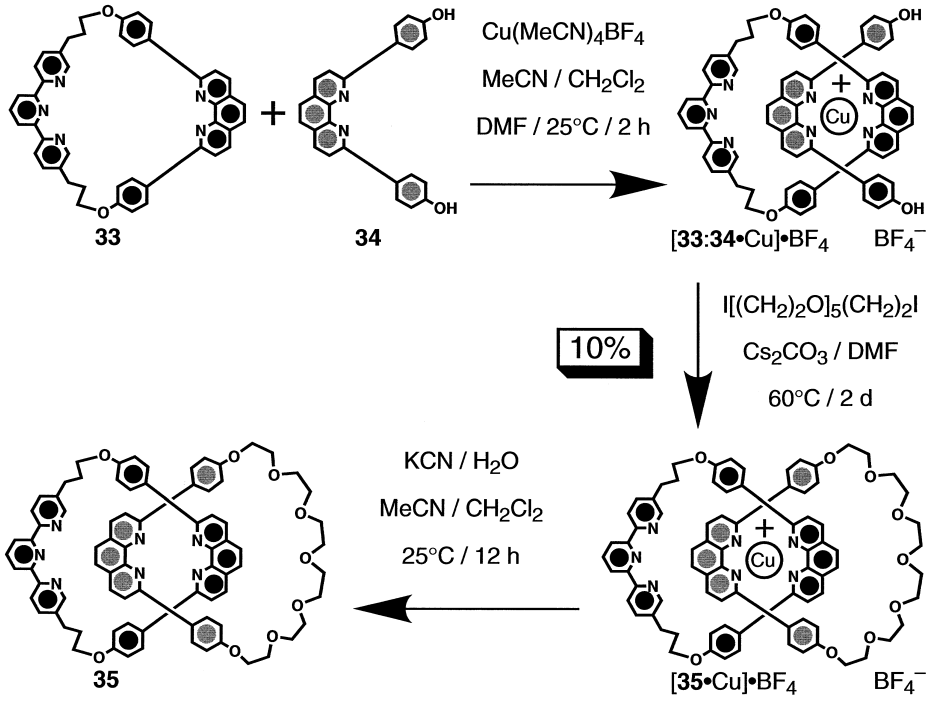

Figure 10.26. The template-directed synthesis of the [2]catenane **35**.

10.25) but their chemical shifts are not affected significantly, indicating that the tetrathiafulvalene unit is not oxidized by **16**. By contrast, the two singlets for H_c are shifted by *c.* –3.0 p.p.m. as the 1,4-dioxybenzene ring becomes encircled by the tetracationic cyclophane. After the reduction of the *o*-chloroanil ring incorporated within the adduct [**16**:**31**]•4PF_6 and the subsequent circumrotation of the macrocyclic polyether, the original singlets associated with H_c are observed ((c) in the inset in Fig. 10.25) once again.

The ability of transition metals to coordinate organic ligands can be exploited [ref. 32] (Fig. 10.26) to template the formation of [2]catenanes. Upon mixing equimolar amounts of the phenanthroline-based ligands **33** and **34** with $Cu(MeCN)_4BF_4$ in solution, the complex [**33**:**34**•Cu]•BF_4 self-assembles spontaneously. Reaction of [**33**:**34**•Cu]•BF_4 with $I[(CH_2)_2O]_5(CH_2)_2I$ gives the [2]catenate [**35**•Cu]•BF_4 in a yield of 10%. Demetalation [ref. 33] can be achieved by treating [**35**•Cu]•BF_4 with KCN in solution to afford the [2]catenane **35** quantitatively. The redox-controlled switching [ref. 34] of the [2]catenate [**35**•Cu]•BF_4 can be realized by oxidation/reduction of the transition metal, since Cu^+ and Cu^{2+} have different coordination requirements. Indeed, Cu^+ prefers tetracoordination while Cu^{2+} is stabilized by pentacoordination.

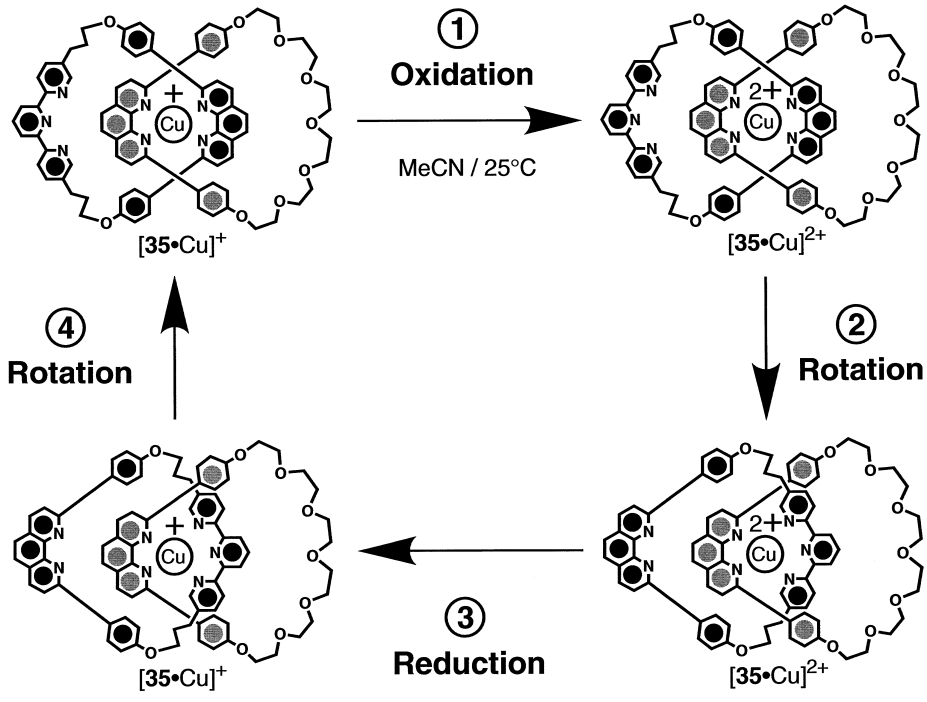

Figure 10.27. The redox-controlled switching of the [2]catenane [**35**•Cu]$^{+}$.

The electrochemical oxidation of [**35**•Cu]$^{+}$ generates (step 1 in Fig. 10.27) a Cu^{2+} center in a tetracoordination environment. As a result, circumrotation of the terpyridine-containing macrocycle through the cavity of the other macrocycle occurs (step 2 in Fig. 10.27) to afford a more stable pentacoordinated Cu^{2+} center. The electrochemical reduction of [**35**•Cu]$^{2+}$ affords (step 3 in Fig. 10.27) a pentacoordinated Cu^{+} center. However, the circumrotation of the terpyridine-containing macrocycle yields back (step 4 in Fig. 10.27) the original co-conformation in which the Cu^{+} center can enjoy its much preferred tetracoordinating environment. The switching of this [2]catenate is accompanied by a change in color from red to green on going from [**35**•Cu]$^{+}$ to [**35**•Cu]$^{2+}$ and *vice versa*. Also, the redox potential for the Cu^{2+}/Cu^{+} semicouple varies from +0.63 V to –0.07 V on going from a tetra- to a pentacoordination environment and *vice versa*.

10.5 Conclusions and future perspectives

As a result of their superstructural and structural properties, [2]pseudorotaxanes and [2]rotaxanes and [2]catenanes, respectively, are ideal candidates for

the design of molecular-sized switches. Indeed, a number of bistable chemical systems, that can be switched reversibly between a *State 0* and a *State 1*, have been realized in the shape of such interpenetrating and interlocked supramolecular and molecular species. In all instances, the switching processes are associated with the relative movement of one of the two interpenetrating or interlocked components relative to the other. These molecular level motions can be induced by chemical, electrochemical, and/or photochemical stimuli (input signal) that alter the recognition properties of an appropriate unit incorporated in one of the two components. In response to the input signal, the chemical system alters its co-conformation and this change can be read spectroscopically (output signal). Although these bistable systems have been synthesized and their switching properties have been characterized fully in solution, considerable progress has to be made to incorporate them into ultra-densely integrated electronic circuits. Methods for their efficient and precise attachment to solid supports need to be developed. Furthermore, techniques to fabricate arrays of interconnected molecular-sized switches and to operate them individually have to be devised. Nonetheless, the remarkable progress achieved so far in the field is extremely encouraging. The recent realization of electronically-configurable logic gates, based on rotaxanes incorporating π-electron deficient dumbbell-shaped components and π-electron rich macrocycles, demonstrates [ref. 35] that electronic circuits made of organic molecules can, indeed, be fabricated.

10.6 References

1. Muller, R. S. and Kamins, T. I. (1986). *Device Electronics for Integrated Circuits*. Wiley, New York.
2. Mitchell, R. J. (1995). *Microprocessor Systems*. Macmillan, London.
3. Jortner, J. and Ratner, M. (Eds.). (1997). *Molecular Electronics*. Blackwell Science, Oxford.
4. (a) Vögtle, F. (1991). *Supramolecular Chemistry*. Wiley, New York. (b) Lehn, J.-M. (1995). *Supramolecular Chemistry*. VCH, Weinheim. (c) Lehn, J.-M., Atwood, J. L., Davies, J. E. D., MacNicol, D. D. and Vögtle, F. (Eds.). (1996). *Comprehensive Supramolecular Chemistry*. Pergamon, Oxford.
5. For reviews on switchable molecular and supramolecular systems, see: (a) Balzani, V. and Scandola, F. (1991). *Supramolecular Photochemistry*. Horwood, Chichester. (b) Balzani, V. (1992). *Tetrahedron* **48**, 10443–10514. (c) Bissell, R. A., de Silva, A. P., Gunaratne, H. Q. N., Lynch, P. L. M., Maguire, G. E. M., McCoy, C. P. and Sandanayake, K. R. A. S. (1993). *Top. Curr. Chem.* **168**, 223–264. (d) de Silva, A. P. and McCoy, C. P. (1994). *Chem. Ind.* 992–996. (e) Fabbrizzi, L. and Poggi, A. (1995). *Chem. Soc. Rev.* **24**, 197–202. (f) Shinkai, S. (1996). *Comprehensive Supramolecular Chemistry* (Atwood, J. L., Davies, J. E. D., Macnicol, D. D. and Vögtle, F., Eds.), Vol. 1, pp. 671–700. Pergamon, Oxford. (g) de Silva, A. P., Gunaratne, H. Q. N., Gunnlaugsson, T., Huxley,

A. J. M., McCoy, C. P., Rademacher, J. T. and Rice, T. E. (1997). *Chem. Rev.* **97**, 1515–1566. (h) Ward, M. D. (1997). *Chem. Ind.*, 640–645. (i) Beer, P. D. (1998). *Acc. Chem. Res.* **31**, 71–80. (j) Boulas, P. L., Gómez-Kaifer, M. and Echegoyen, L. (1998). *Angew. Chem., Int. Ed. Engl.* **37**, 216–247. (k) Bryce, M. R. (1999). *Adv. Mater.* **11**, 11–23. (l) Niemz, A. and Rotello, V. M. (1999). *Acc. Chem. Res.* **32**, 42–52.

6. For monographs and reviews on molecules incorporating interlocked components, see: (a) Schill, G. (1971). *Catenanes, Rotaxanes and Knots*. Academic Press, New York. (b) Walba, D. M. (1985). *Tetrahedron* **41**, 3161–3212. (c) Dietrich-Buchecker, C. O. and Sauvage, J.-P. (1987). *Chem. Rev.* **87**, 795–810. (d) Dietrich-Buchecker, C. O. and Sauvage, J.-P. (1991). *Bioorg. Chem. Front.* **2**, 195–248. (e) Chambron, J.-C., Dietrich-Buchecker, C. O. and Sauvage, J.-P. (1993). *Top. Curr. Chem.* **165**, 131–162. (f) Gibson, H. W. and Marand, H. (1993). *Adv. Mater.* **5**, 11–21. (g) Gibson, H. W., Bheda, M. C. and Engen, P. T. (1994). *Prog. Polym. Sci.* **19**, 843–945. (h) Amabilino, D. B., Parsons, I. W. and Stoddart, J. F. (1994). *Trends Polym. Sci.* **2**, 146–152. (i) Amabilino, D. B. and Stoddart, J. F. (1995). *Chem. Rev.* **95**, 2725–2828. (j) Gibson, H. W. (1996). *Large Ring Molecules* (Semlyen, J. A., Ed.), pp. 191–202. Wiley, New York. (k) Belohradsky, M., Raymo, F. M. and Stoddart, J. F. (1996). *Collect. Czech. Chem. Commun.* **61**, 1–43. (l) Raymo, F. M. and Stoddart, J. F. (1996). *Trends Polym. Sci.* **4**, 208–211. (m) Belohradsky, M., Raymo, F. M. and Stoddart, J. F. (1997). *Collect. Czech. Chem. Commun.* **62**, 527–557. (n) Jäger, R. and Vögtle, F. (1997). *Angew. Chem., Int. Ed. Engl.* **36**, 930–944. (o) Clarkson, G. J., Leigh, D. A. and Smith, R. A. (1998). *Curr. Op. Solid State Mater. Sci.* **3**, 579–584. (p) Leigh, D. A. and Murphy, A. (1999). *Chem. Ind.* 178–183. (q) Breault, G. A., Hunter, C. A. and Mayers, P. C. (1999). *Tetrahedron* **55**, 5265–5293. (r) Dietrich-Buckecher, C. O. and Sauvage, J.-P. (Eds.). (1999). *Catenanes, Rotaxanes and Knots.* VCH-Wiley, Weinheim. (p) Raymo, F. M. and Stoddart, J. F. (1999). *Chem. Rev.* **99**, 1643–1663.
7. For reviews on switchable pseudorotaxanes, rotaxanes and catenanes, see: (a) Benniston, A. C. (1996). *Chem. Soc. Rev.* **25**, 427–435. (b) Balzani, V., Gómez-López, M. and Stoddart, J. F. (1998). *Acc. Chem. Res.* **31**, 405–414. (c) Sauvage, J.-P. (1998). *Acc. Chem. Res.* **31**, 611–619. (d) Sauvage, J.-P. (1998). *Bull. Pol. Acad. Sci. Chem.* **46**, 289–307. (e) Chambron, J.-C. and Sauvage, J.-P. (1998). *Chem. Eur. J.* **4**, 1362–1366. (f) Kaifer, A. E. (1999). *Acc. Chem. Res.* **32**, 62–71.
8. For examples of molecular machines based of the relative movements of their components, see: (a) Iwamura, H. and Mislow, K. (1988). *Acc. Chem. Res.* **21**, 175–182. (b) Mislow, K. (1989). *Chemtracts* **2**, 151–174. (c) Kelly, T. R., Bowyer, M. C., Bhaskar, K. V., Bebbington, D., Gracia, A., Lang, F., Kim, M. H. and Jette, M. P. (1994). *J. Am. Chem. Soc.* **116**, 3657–3658. (d) Bedard, T. C. and Moore, J. S. (1997). *J. Am. Chem. Soc.* **117**, 10662–10671. (e) Canevet, C., Libman, J. and Shanzer, A. (1996). *Angew. Chem., Int. Ed. Engl.* **35**, 2657–2660. (f) de Santis, G., Fabbrizzi, L., Iacopino, D., Pallavicini, P., Perotti, A. and Poggi, A. (1997). *Inorg. Chem.* **36**, 827–832. (g) Willner, I. (1997). *Acc. Chem. Res.* **30**, 347–356. (h) Ikeda, A., Tsudera, T. and Shinkai, S. (1997). *J. Org. Chem.* **62**, 3568–3574. (i) Kelly, T. R., Tellita, I. and Sestelo, J. P. (1997). *Angew. Chem., Int. Ed. Engl.* **36**, 1866–1868. (j) Deans, R., Niemz, A., Breinlinger, E. C. and Rotello, V. M. (1997). *J. Am. Chem. Soc.* **119**, 10863–10864. (k) Stevens, A. N. and Richards, C. J. (1997). *Tetrahedron Lett.* **38**, 7805–7808. (l) Malpass, J. R., Sun, G., Fawcett, J. and Wartner, R. N.

(1998). *Tetrahedron Lett.* **38**, 3083–3086. (m) Bryce, M. R., de Miguel, P. and Devonport, W. (1998). *J. Chem. Soc., Chem. Commun.,* 2565–2566. (n) Takashita, M. and Irie, M. (1998). *J. Org. Chem.* **63**, 6643–6649. (o) Archut, A., Azzellini, G. C., Balzani, V., De Cola, L. and Vögtle, F. (1998). *J. Am. Chem. Soc.* **120**, 12187–12191. (p) de Silva, A. P., Dixon, I. M., Gunaratne, H. Q. N., Gunnlaugsson, T., Maxwell, P. R. S. and Rice, T. E. (1999). *J. Am. Chem. Soc.* **121**, 1393–1394. (q) Fabbrizzi, L., Gatti, F., Pallavicini, P. and Zambarbieri, E. (1999). *Chem. Eur. J.* **5**, 682–690.

9. For the binding properties of **1**•4PF_6, see: (a) Ashton, P. R., Goodnow, T. T., Kaifer, A. E., Reddington, M. V., Slawin, A. M. Z., Spencer, N., Stoddart, J. F., Vicent, C. and Williams, D. J. (1989). *Angew. Chem., Int. Ed. Engl.* **28**, 1396–1399. (b) Anelli, P.-L., Ashton, P. R., Ballardini, R., Balzani, V., Delgado, M., Gandolfi, M. T., Goodnow, T. T., Kaifer, A. E., Philp, D., Pietraszkiewicz, M., Prodi, L., Reddington, M. V., Slawin, A. M. Z., Spencer, N., Stoddart, J. F., Vicent, C. and Williams, D. J. (1992). *J. Am. Chem. Soc.* **114**, 193–218. (c) Gillard, R. E., Stoddart, J. F., White, A. J. P., Williams, B. J. and Williams, D. J. (1996). *J. Org. Chem.* **61**, 4504– 4505. (d) Asakawa, M., Dehaen, W., L'abbé, G., Menzer, S., Nouwen, J., Raymo, F. M., Stoddart, J. F. and Williams, D. J. (1996). *J. Org. Chem.* **61**, 9591–9595. (e) Ballardini, R., Balzani, V., Brown, C. L., Credi, A., Gillard, R. E., Montalti, M., Philp, D., Stoddart, J. F., Venturi, M., White, A. J. P., Williams, B. J. and Williams, D. J. (1997). *J. Am. Chem. Soc.* **119**, 12 503–12 513.
10. For accounts and reviews on the use of this recognition motif to template the synthesis of catenanes and rotaxanes, see: (a) Amabilino, D. B. and Stoddart, J. F. (1993). *Pure Appl. Chem.* **65**, 2351–2359. (b) Pasini, D., Raymo, F. M. and Stoddart, J. F. (1995). *Gazz. Chim. Ital.* **125**, 431–435. (c) Langford, S. J. and Stoddart, J. F. (1996). *Pure Appl. Chem.* **68**, 1255–1260. (d) Amabilino, D. B., Raymo, F. M. and Stoddart, J. F. (1996). *Comprehensive Supramolecular Chemistry* (Hosseini, M. W. and Sauvage, J.-P., Eds.), Vol. 9, pp. 85–130. Pergamon, Oxford. (e) Raymo, F. M. and Stoddart, J. F. (1997). *Pure Appl. Chem.* **69**, 1987–1997. (f) Gillard, R. E., Raymo, F. M. and Stoddart, J. F. (1997). *Chem. Eur. J.* **3**, 1933–1940. (g) Raymo, F. M. and Stoddart, J. F. (1998). *Chemtracts* **11**, 491–511.
11. For accounts and reviews on [C−H$\cdots$O] hydrogen bonds, see: (a) Desiraju, G. R. (1991). *Acc. Chem. Res.* **24**, 290–296. (b) Desiraju, G.R. (1996) *Acc. Chem. Res.* **29**, 441–449. (c) Steiner, T. (1997). *J. Chem. Soc., Chem. Commun.*, 727–734. (d) Berger, I. and Egli, M. (1997). *Chem. Eur. J.* **3**, 1400–1404.
12. For accounts and reviews on [$\pi\cdots\pi$] stacking interactions, see: (a) Schwartz, M. H. (1990). *J. Inclusion Phenom.* **9**, 1–35. (b) Williams, J. H. (1993). *Acc. Chem. Res.* **26**, 593–598. (c) Hunter, C. A. (1993). *Angew. Chem., Int. Ed. Engl.* **32**, 1584–1586. (d) Hunter, C. A. (1993). *J. Mol. Biol.* **230**, 1025–1054. (e) Dahl, T. (1994). *Acta Chem. Scand.* **48**, 95–116. (f) Cozzi, F. and Siegel, J. S. (1995). *Pure Appl. Chem.* **67**, 683–689. (g) Claessens, C. G. and Stoddart, J. F. (1997). *J. Phys. Org. Chem.* **10**, 254–272.
13. For accounts and reviews on template-directed syntheses, see: (a) Busch, D. H. and Stephenson, N. A. (1990). *Coord. Chem. Rev.* **100**, 119–154. (b) Lindsey, J. S. (1991). *New J. Chem.* **15**, 153–180. (c) Whitesides, G. M., Mathias, J. P. and Seto, C. T. (1991). *Science* **254**, 1312–1319. (d) Philp, D. and Stoddart, J. F. (1991). *Synlett* 445–458. (e) Busch, D. H. (1992). *J. Inclusion Phenom.* **12**, 389–395. (f) Anderson, S., Anderson, H. L. and Sanders, J. K. M. (1993). *Acc.*

Chem. Res. **26**, 469–475. (g) Cacciapaglia, R. and Mandolini, L. (1993). *Chem. Soc. Rev.* **22**, 221–231. (h) Hoss, R. and Vögtle, F. (1994). *Angew. Chem., Int. Ed. Engl.* **33**, 375–384. (i) Schneider, J. P. and Kelly, J. W. (1995). *Chem. Rev.* **95**, 2169–2187. (j) Philp, D. and Stoddart, J. F. (1996). *Angew. Chem., Int. Ed. Engl.* **35**, 1155–1196. (k) Raymo, F. M. and Stoddart, J. F. (1996). *Pure Appl. Chem.* **68**, 313–322. (l) Fyfe, M. C. T. and Stoddart, J. F. (1997). *Acc. Chem. Res.* **30**, 393–401. (m) Hubin, T. J., Kolchinski, A. G., Vance, A. L. and Busch, D. L. (1999). *Adv. Supramol. Chem.* **5**, 237–357.

14. Matthews, O. A., Raymo, F. M., Stoddart, J. F., White, A. J. P. and Williams, D. J. (1998). *New J. Chem.* 1131–1134.
15. For related examples of switchable [2]pseudorotaxanes, see: (a) Ashton, P. R., Gómez-López, M., Iqbal, S., Preece, J. A. and Stoddart, J. F. (1997). *Tetrahedron Lett.* **38**, 3635–3638. (b) Asakawa, M., Iqbal, S., Stoddart, J. F. and Tinker, N. D. (1996). *Angew. Chem., Int. Ed. Engl.* **35**, 976–978. (c) Ashton, P. R., Iqbal, S., Stoddart, J. F. and Tinker, N. D. (1996). *J. Chem. Soc., Chem. Commun.,* 479–481. (d) Montalti, M., Ballardini, R., Prodi, L. and Balzani, V. (1996). *J. Chem. Soc*., *Chem. Commun.*, 2011–2012. (e) Ashton, P. R., Ballardini, R., Balzani, V., Gómez-López, M., Lawrence, S. E., Martínez-Díaz, M.-V., Montalti, M., Piersanti, A., Prodi, L., Stoddart, J. F. and Williams, D. J. (1997). *J. Am. Chem. Soc.* **119**, 10641–10651. (f) Montalti, M. and Prodi, L. (1998). *J. Chem. Soc., Chem. Commun.*, 1461–1462. (g) Ashton, P. R., Ballardini, R., Balzani, V., Fyfe, M. C. T., Gandolfi, M. T., Martínez-Díaz, M. V., Morosini, M., Schiavo, C., Shibata, K., Stoddart, J. F., White, A. J. P. and Williams, D. J. (1998). *Chem. Eur. J.* **4**, 2332–2341.
16. Asakawa, M., Ashton, P. R., Balzani, V., Boyd, S. E., Credi, A., Mattersteig, G., Menzer, S., Montalti, M., Raymo, F. M., Ruffilli, C., Stoddart, J. F., Venturi, M. and Williams, D. J. (1999). *Eur. J. Org. Chem.*, 985–994.
17. For related examples of switchable [2]pseudorotaxanes, see: (a) Diaz, A., Quintela, P. A., Schuette, J. M. and Kaifer, A.E. (1988). *J. Phys. Chem.* **92**, 3537–3542. (b) Fonseca, R. J., Colina, J. T. and Smith, D. K. (1992). *J. Electroanal. Chem.* **340**, 341–348. (c) Smith, E. A., Lilienthal, R. R., Fonseca, R. J. and Smith, D. K. (1994). *Anal. Chem.* **66**, 3013–3020. (d) Córdova, E., Bissell, R. A. and Kaifer, A. E. (1995). *J. Org. Chem.* **60**, 1033–1038. (e) Devonport, W., Blower, M. A., Bryce, M. R. and Goldenberg, L. M. (1997). *J. Org. Chem.* **62**, 885–887. (f) Asakawa, M., Ashton, P. R., Balzani, V., Credi, A., Mattersteig, G., Matthews, O. A., Montalti, M., Spencer, N., Stoddart, J. F. and Venturi, M. (1997). *Chem. Eur. J.* **3**, 1992–1996. (g) Ashton, P. R., Ballardini, R., Balzani, V., Boyd, S. E., Credi, A., Gandolfi, M. T., Gómez-López, M., Iqbal, S., Philp, D., Preece, J. A., Prodi, L., Ricketts, H. G., Stoddart, J. F., Tolley, M. S., Venturi, M., White, A. J. P. and Williams, D. J. (1997). *Chem. Eur. J.* **3**, 152–168. (h) Collin, J.-P., Gaviña, P. and Sauvage, J.-P. (1996). *J. Chem. Soc., Chem. Commun.*, 2005–2006. (i) Mirzoian, A. and Kaifer, A.E. (1997). *Chem. Eur. J.* **3**, 1052–1058. (j) Castro, R., Godinez, L. A., Criss, C. M. and Kaifer, A. E. (1997). *J. Org. Chem.* **62**, 4928–4935.
18. Asakawa, M., Ashton, P. R., Balzani, V., Brown, C. L., Credi, A., Matthews, O. A., Newton, S. P., Raymo, F. M., Shipway, A. N., Spencer, N., Quick, A., Stoddart, J. F., White, A. J. P. and Williams, D. J. (1999). *Chem. Eur. J.* **5**, 860–875.
19. For related examples of switchable [2]pseudorotaxanes, see: (a) Ballardini, R., Balzani, V., Gandolfi, M. T., Prodi, L., Venturi, M., Philp, D., Ricketts, H. G.

and Stoddart, J. F. (1993). *Angew. Chem., Int. Ed. Engl.* **32**, 1301–1303. (b) Seiler, M., Dürr, H., Willner, I., Joselevich, E., Doron, A. and Stoddart, J. F. (1994). *J. Am. Chem. Soc.* **116**, 3399–3404. (c) Kropf, M., Joselevich, E., Dürr, H. and Willner, I. (1996). *J. Am. Chem. Soc.* **118**, 655–665. (d) David, E., Born, R., Kaganer, E., Joselevich, E., Dürr, H. and Willner, I. (1997). *J. Am. Chem. Soc.* **119**, 7778–7790. (e) Benniston, A. C., Harriman, A. and Yufit, D. S. (1997). *Angew. Chem., Int. Ed. Engl.* **36**, 2356–2358. (f) Ashton, P. R., Balzani, V., Kocian, O., Prodi, L., Spencer, N. and Stoddart, J. F. (1998). *J. Am. Chem. Soc.* **120**, 11190–11191.

20. Balzani, V., Credi, A., Mattersteig, G., Matthews, O. A., Raymo, F. M., Stoddart, J. F., Venturi, M., White, A. J. P. and Williams, D. J. (2000). *J. Org. Chem*. **65**, 1924–1936.
21. For related examples of switchable [2]pseudorotaxanes, see: (a) Ballardini, R., Balzani, V., Credi, A., Gandolfi, M. T., Langford, S. J., Menzer, S., Prodi, L., Stoddart, J. F., Venturi, M. and Williams, D. J. (1996). *Angew. Chem., Int. Ed. Engl.* **35**, 978–981. (b) Credi, A., Balzani, V., Langford, S. J. and Stoddart, J. F. (1997). *J. Am. Chem. Soc.* **119**, 2679–2681.
22. Credi, A., Balzani, V., Langford, S. J ., Montalti, M., Raymo, F. M. and Stoddart, J. F. (1998). *New J. Chem.*, 1061–1065.
23. Ashton, P. R., Balzani, V., Becher, J., Credi, A., Fyfe, M. C. T., Mattersteig, G., Menzer, S., Nielsen, M. B., Raymo, F. M., Stoddart, J. F., Venturi, M. and Williams, D. J. (1999). *J. Am. Chem. Soc.* **121**, 3951–3957.
24. Bissell, R. A., Córdova, E., Kaifer, A. E. and Stoddart, J. F. (1994). *Nature* **369**, 133–137.
25. For related examples of switchable [2]rotaxanes, see: (a) Collin, J.-P., Gaviña, P. and Sauvage, J.-P. (1997). *New J. Chem.* **21**, 525–528. (b) Gaviña, P. and Sauvage, J.-P. (1997). *Tetrahedron Lett.* **38**, 3521–3524 (b) Armaroli, N., Balzani, V., Collin, J.-P., Gaviã, P., Sauvage, J.–P. and Ventura, B. (1999). *J. Am. Chem. Soc.* **121**, 4397–4408.
26. (a) Martínez-Díaz, M.-V., Spencer, N. and Stoddart, J. F. (1997). *Angew. Chem., Int. Ed. Engl.* **36**, 1904–1907. (b) Ashton, P. R., Ballardini, R., Balzani, V., Baxter, I., Credi, A., Fyfe, M. C. T., Gandolfi, M. T., Gómez-López, M., Martínez-Díaz, M.-V., Piersanti, A., Spencer, N., Stoddart, J. F., Venturi, M., White, A. J. P. and Williams, D. J. (1998). *J. Am. Chem. Soc.* **120**, 11932–11942.
27. For a definition of the term 'co-conformation', see: Fyfe, M. C. T., Glink, P. T., Menzer, S., Stoddart, J. F., White, A. J. P. and Williams, D. J. (1997). *Angew. Chem., Int. Ed. Engl.* **36**, 2068–2070.
28. Murakami, H., Kawabuchi, A., Kotoo, K., Kunitake, M. and Nakashima, N. (1997). *J. Am. Chem. Soc.* **119**, 7605–7606.
29. For related examples of switchable [2]rotaxanes, see: (a) Benniston, A. C. and Harriman, A. (1993). *Angew. Chem.* **32**, 1459–1461. (b) Benniston, A. C., Harriman, A. and Lynch, V. M. (1994). *Tetrahedron Lett.* **35**, 1473–1476. (c) Benniston, A. C., Harriman, A. and Lynch, V. M. (1995). *J. Am. Chem. Soc.* **117**, 5275–5291.
30. Asakawa, M., Ashton, P. R., Balzani, V., Credi, A., Hamers, C., Mattersteig, G., Montalti, M., Shipway, A. N., Spencer, N., Stoddart, J. F., Tolley, M. S., Venturi, M., White, A. J. P. and Williams, D. J. (1998). *Angew. Chem., Int. Ed. Engl.* **37**, 333–337.
31. For related examples of switching [2]catenanes, see: (a) Gunter, M. J. and Johnston, M. R. (1994). *J. Chem. Soc., Chem. Commun.*, 829–830. (b) Ashton,

P. R., Ballardini, R., Balzani, V., Gandolfi, M. T., Marquis, D. J.-F., Pérez-García, L., Stoddart, J. F. and Venturi, M. (1994). *J. Chem. Soc., Chem. Commun.*, 177–180. (c) Ballardini, R., Balzani, V., Credi, A., Gandolfi, M. T., Prodi, L., Venturi, M., Pérez-García, L. and Stoddart, J. F. (1995). *Gazz. Chim. Ital.* **125**, 353–359. (d) Ashton, P. R., Ballardini, R., Balzani, V., Credi, A., Gandolfi, M. T., Menzer, S., Pérez-García, L., Prodi, L., Stoddart, J. F., Venturi, M. White, A. J. P. and Williams, D. J. (1995). *J. Am. Chem. Soc.* **117**, 11171–11197.

32. (a) Livoreil, A., Dietrich-Buchecker, C. O. and Sauvage, J.-P. (1994). *J. Am. Chem. Soc.* **116**, 9399–9400. (b) Baumann, F., Livoreil, A., Kaim, W. and Sauvage, J.-P. (1997). *J. Chem. Soc., Chem. Commun.*, 35–36. (c) Livoreil, A., Sauvage, J.-P., Armaroli, N., Balzani, V., Flamigni, L. and Ventura, B. (1997). *J. Am. Chem. Soc.* **119**, 12114–12124.
33. The terms '[2]catenate' and '[2]catenand' are often used to indicate the metalated and demetalated forms, respectively, of [2]catenanes such as **35**. In related [2]catenanes, the demetalation/metalation processes are accompanied by the circumrotation of one macrocyclic component through the cavity of the other. These systems can be regarded as chemically controllable molecular switches. For examples, see: (a) Dietrich-Buchecker, C. O., Sauvage, J.-P. and Kern, J.-M. (1984). *J. Am. Chem. Soc.* **106**, 3043–3045. (b) Albrecht-Gary, A.-M., Saad, Z., Dietrich-Buchecker, C. O. and Sauvage, J.-P. (1985). *J. Am. Chem. Soc.* **107**, 3205–3209. (c) Cesario, M., Dietrich-Buchecker, C. O., Guilhem, J., Pascard, C. and Sauvage, J.-P. (1985). *J. Chem. Soc., Chem. Commun.*, 244–247. (d) Cesario, M., Dietrich-Buchecker, C. O., Edel, A., Guilhem, J., Kintzinger, J.-P., Pascard, C. and Sauvage, J.-P. (1986). *J. Am. Chem. Soc.* **108**, 6250–6254. (e) Albrecht-Gary, A.-M., Dietrich-Buchecker, C. O., Saad, Z., Sauvage, J.-P. and Weiss, J. (1986). *J. Chem. Soc. Chem. Commun.*, 1325–1327. (f) Dietrich-Buchecker, C. O., Sauvage, J.-P. and Weiss, J. (1986). *Tetrahedron Lett.* **27I**, 2257–2260. (g) Albrecht-Gary, A.-M., Dietrich-Buchecker, C. O., Saad, Z. and Sauvage, J.-P. (1988). *J. Am. Chem. Soc.* **110**, 1467–1472. (h) Dietrich-Buchecker, C. O., Sauvage, J.-P. (1990). *Tetrahedron.* **46**, 503–512. (i) Albrecht-Gary, A.-M., Dietrich-Buchecker, C. O., Saad, Z. and Sauvage, J.-P. (1992). *J. Chem. Soc., Chem. Commun.*, 280–282. (j) Armaroli, N., De Cola, L., Balzani, V., Sauvage, J.-P., Dietrich-Buchecker, C. O., Kern, J.-M. and Bailal, A. (1992). *J. Chem. Soc., Dalton Trans.*, 3242–3246. (k) Sauvage, J.-P. and Weiss, J. (1985). *J. Am. Chem. Soc.* **107**, 6108–6110. (l) Dietrich-Buchecker, C. O., Khemiss, A. and Sauvage, J.-P. (1986). *J. Chem. Soc. Chem., Commun.* 1376–1378. (m) Armaroli, N., Balzani, V., De Cola, L., Hemmert, C. and Sauvage, J.-P. (1994). *New J. Chem.* **18**, 775–782. (n) Amabilino, D. B., Dietrich-Buchecker, C. O., Livoreil, A., Pérez-García, L., Sauvage, J.-P. and Stoddart, J. F. (1996). *J. Am. Chem. Soc.* **118**, 3905–3913.
34. For a related redox switchable [2]catenane, see: Cárdenas, D. J., Livoreil, A. and Sauvage, J.-P. (1996). *J. Am. Chem. Soc.* **118**, 11980–11981.
35. (a) Collier, C. P., Wong, E. W., Behloradsky, M., Raymo, F. M., Stoddart, J. F., Kuekes, P. J., Williams, R. S. and Heath, J. R. (1999). *Science*, **285**, 391–394. (b) Wong, E. W., Collier, C. P., Behloradsky, M., Raymo, F. M., Stoddart, J. F. and Heath, J. R. (2000). *J. Am. Chem. Soc*. **122**, 5831–5840. (c) see also, Collier, C. P., Mattersteig, G., Wong, E. W., Luo, Y., Beverly, K., Sampaio, J., Raymo, F. M., Stottart, J. F. and Heath, J. R. (2000). *Science* **289**, 1172–1175.